



Evidence for transverse momentum and pseudorapidity dependent event plane fluctuations in PbPb and pPb collisions

The CMS Collaboration*

Abstract

A systematic study of the factorization of long-range azimuthal two-particle correlations into a product of single-particle anisotropies is presented as a function of p_T and η of both particles, and as a function of the particle multiplicity in PbPb and pPb collisions. The data were taken with the CMS detector for PbPb collisions at $\sqrt{s_{NN}} = 2.76$ TeV and pPb collisions at $\sqrt{s_{NN}} = 5.02$ TeV, covering a very wide range of multiplicity. Factorization is observed to be broken as a function of both particle p_T and η . When measured with particles of different p_T , the magnitude of the factorization breakdown for the second Fourier harmonic reaches 20% for very central PbPb collisions but decreases rapidly as the multiplicity decreases. The data are consistent with viscous hydrodynamic predictions, which suggest that the effect of factorization breaking is mainly sensitive to the initial-state conditions rather than to the transport properties (e.g., shear viscosity) of the medium. The factorization breakdown is also computed with particles of different η . The effect is found to be weakest for mid-central PbPb events but becomes larger for more central or peripheral PbPb collisions, and also for very high-multiplicity pPb collisions. The η -dependent factorization data provide new insights to the longitudinal evolution of the medium formed in heavy ion collisions.

Published in Physical Review C as doi:10.1103/PhysRevC.92.034911.

1 Introduction

The goal of experiments with heavy ion collisions at ultra-relativistic energies is to study nuclear matter under extreme conditions. By studying the azimuthal anisotropy of emitted particles in such collisions, experiments at the Relativistic Heavy Ion Collider at BNL (RHIC) indicated that a strongly-coupled hot and dense medium is created, which exhibits a strong collective flow behavior [1–4]. At the significantly higher collision energies achieved at the Large Hadron Collider (LHC), the collective phenomena of this quark gluon plasma have also been studied in great detail [5–13].

The collective expansion of the hot medium in heavy ion collisions can be described by hydrodynamic flow models. Motivated by such models, the azimuthal distribution of emitted particles can be characterized by the Fourier components of the hadron yield distribution in azimuthal angle (ϕ) [14–16],

$$\frac{dN}{d\phi} \propto 1 + 2 \sum_n v_n \cos[n(\phi - \Psi_n)]. \quad (1)$$

Here, the Fourier coefficients, v_n , characterize the strength of the anisotropic flow, while the azimuthal flow orientation is represented by the corresponding “event plane” angle, Ψ_n , the direction of maximum final-state particle density. The event plane angles are related to the event-by-event spacial distribution of the participating nucleons in the initial overlap region. The most widely studied and typically also strongest form of anisotropic flow is the second Fourier component, v_2 , called “elliptic flow”. The elliptic flow event plane, Ψ_2 , is correlated with the “participant plane” given by the beam direction and the shorter axis of the approximately elliptical nucleon overlap region. Because of event-by-event fluctuations, higher-order deformations or eccentricities of the initial geometry can also be induced, which lead to higher-order Fourier harmonics ($v_n, n \geq 3$) in the final state with respect to their corresponding event plane angles, Ψ_n [17]. Studies of azimuthal anisotropy harmonics provide important information on the fundamental transport properties of the medium, e.g., the ratio of shear viscosity to entropy density, η/s [18–20].

A commonly used experimental method to determine the single-particle azimuthal anisotropy harmonics, v_n , is the measurement of two-particle azimuthal correlations [14–16, 21]. The azimuthal distribution of particle pairs as a function of their relative azimuthal angle $\Delta\phi$ can also be characterized by its Fourier components,

$$\frac{dN^{\text{pair}}}{d\Delta\phi} \propto 1 + 2 \sum_n V_{n\Delta} \cos(n\Delta\phi). \quad (2)$$

If the dominant source of final-state particle correlations is collective flow, the two-particle Fourier coefficients, $V_{n\Delta}$, are commonly expected to follow the factorization relation:

$$V_{n\Delta} = v_n^a v_n^b, \quad (3)$$

where v_n^a and v_n^b represent the single-particle anisotropy harmonics for a pair of particles (a and b) in the event. The particle pairs can be selected from the same or different transverse momentum (p_T) and pseudorapidity (η) ranges. Here, a key assumption is that the event plane angle Ψ_n in Eq. (1) is a global phase angle for all particles of the entire event, which is canceled when taking the azimuthal angle difference between two particles. As a result, the flow-driven $\Delta\phi$ distribution in Eq. (2) has no dependence on Ψ_n . The most common approach to obtain the single-particle v_n in the two-particle method is to fix one particle in a wide p_T (η) region and measure $V_{n\Delta}$ by only varying p_T (η) of the other particle to determine v_n as a function of p_T (η).

However, a significant breakdown of the factorization assumption, up to about 20%, was recently observed for pairs of particles, separated by more than 2 units in η , from different p_T ranges in ultra-central (0–0.2% centrality) PbPb collisions [13]. The centrality in heavy ion collisions is defined as a fraction of the total inelastic PbPb cross section, with 0% denoting the most central collisions. While nonflow correlations (such as back-to-back jets) have been speculated to possibly account for this effect, contributions of those short-range correlations to the collective anisotropy are less dominant in high-multiplicity events as the total number of particles increases [22]. It was then realized that in hydrodynamic models the assumption of factorization does not hold in general because of fluctuations in the initial overlap region of two nuclei [23, 24]. In each event, due to local perturbations in the energy density distribution generating a pressure gradient that drives particles in random directions with differing boosts, the resulting event plane angles found with final-state particles from different p_T ranges may fluctuate with respect to each other (although still correlated with the initial participant plane). This effect of initial-state fluctuations thus breaks the factorization relation of Eq. (3), which assumes a unique event plane angle for all particles in an event. As a result, the precise meaning of previous single-particle v_n results should be reinterpreted as being with respect to the event plane determined with particles over a specific, usually wide, p_T range. Quantitative studies of the factorization breakdown effect as a function of p_T could place stringent constraints on the spatial scale (or granularity) of the fluctuations in the initial state of heavy ion collisions, especially along the radial direction [25–27].

The recent observation of long-range near-side ($\Delta\phi \sim 0$) two-particle correlations in pp [28] and pPb [29–31] collisions raised the question of whether hydrodynamic flow is developed also in these small collision systems. The extracted v_n harmonics in pPb collisions have been studied in detail as a function of p_T and event multiplicity [22, 32]. The initial-state geometry of a pPb collision is expected to be entirely driven by fluctuations. If the observed long-range correlations in such collisions indeed originate from hydrodynamic flow, the effect of factorization breakdown should also be observed in the data and described by hydrodynamic models. Since the initial-state geometries of both high-multiplicity pPb and ultra-central PbPb collisions are dominated by fluctuations, it is of great interest to investigate whether the magnitude of factorization breakdown is similar in these two systems.

Furthermore, the factorization breakdown in η is sensitive to event plane fluctuations at different η [23]. This phenomenon has been investigated in hydrodynamic and parton transport models [33–36]. The observation and study of this effect will provide new insights into the dynamics of longitudinal expansion of the hot quark and gluon medium, and serves as an ideal test ground of three-dimensional hydrodynamic models.

This paper presents a comprehensive investigation of the factorization breakdown effect in two-particle azimuthal Fourier harmonics in PbPb (pPb) collisions at $\sqrt{s_{NN}} = 2.76$ (5.02) TeV, to search for evidence of p_T - and η -dependent event plane fluctuations. The Fourier harmonics of two-particle azimuthal correlations are extracted for pairs with $|\Delta\eta| > 2$ as a function of p_T and η of both particles in a pair. The results are presented over a wide range of centrality or event multiplicity classes, and are compared with hydrodynamic models in PbPb and pPb collisions. As the p_T - and η -dependent aspects of factorization breakdown probe system dynamics in the transverse and longitudinal directions, respectively, an assumption is made that the dependence on each variable can be studied independently by averaging over the other, and two different analysis techniques are applied. These two aspects of the analysis are described in Sections 4 and 5 separately, including the analysis procedures and results.

2 Experimental setup and data sample

A comprehensive description of the Compact Muon Solenoid (CMS) detector at the CERN LHC, together with a definition of the coordinate system used and the relevant kinematic variables, can be found in Ref. [37]. The main detector sub-system used in this paper is the tracker, located in a superconducting solenoid of 6 m internal diameter, providing a magnetic field of 3.8 T. The tracker consists of 1440 silicon pixel and 15 148 silicon strip detector modules, covering the pseudorapidity range $|\eta| < 2.5$. For hadrons with $p_T \approx 1 \text{ GeV}/c$ and $|\eta| \approx 0$, the impact parameter resolution is approximately $100 \mu\text{m}$ and the p_T resolution is 0.8%.

The electromagnetic calorimeter (ECAL) and the hadron calorimeter (HCAL) are also located inside the solenoid. The ECAL consists of 75 848 lead tungstate crystals, arranged in a quasi-projective geometry and distributed in a barrel region ($|\eta| < 1.48$) and two endcaps that extend to $|\eta| = 3.0$. The HCAL barrel and endcaps are sampling calorimeters composed of brass and scintillator plates, covering $|\eta| < 3.0$. In addition, CMS has an extensive forward calorimetry, in particular two steel/quartz-fiber Cherenkov hadronic forward (HF) calorimeters, which cover the pseudorapidity range $2.9 < |\eta| < 5.2$. The HF calorimeters are segmented into towers, each of which is a two-dimensional cell with a granularity of 0.5 in η and 0.349 radians in ϕ . A set of scintillator tiles, the beam scintillator counters (BSC), are mounted on the inner side of the HF calorimeters and are used for triggering and beam-halo rejection. The BSCs cover the range $3.23 < |\eta| < 4.65$. The detailed Monte Carlo (MC) simulation of the CMS detector response is based on GEANT4 [38].

The data sample used in this analysis was collected with the CMS detector during the LHC PbPb run in 2011 and pPb run in 2013. The total integrated luminosity of the data sets is about $159 \mu\text{b}^{-1}$ for PbPb, and 35 nb^{-1} for pPb. During the pPb run, the beam energies were 4 TeV for protons and 1.58 TeV per nucleon for lead nuclei, resulting in a center-of-mass energy per nucleon pair of 5.02 TeV. As a result of the energy difference between the colliding beams, the nucleon-nucleon center-of-mass in the pPb collisions is not at rest in the laboratory frame. Massless particles emitted at $\eta_{\text{cm}} = 0$ in the nucleon-nucleon center-of-mass frame will be detected at $\eta = -0.465$ or 0.465 (clockwise or counterclockwise proton beam) in the laboratory frame.

3 Selection of events and tracks

Online triggers, offline event selections, track reconstruction and selections are identical to those used in previous analyses of PbPb and pPb data [13, 22] and are briefly outlined in the following sections.

3.1 PbPb data

Minimum bias PbPb events were selected using coincident trigger signals from both ends of the detector in either BSCs or the HF calorimeters. Events due to detector noise, cosmic rays, out-of-time triggers, and beam backgrounds were suppressed by requiring a coincidence of the minimum bias trigger with bunches colliding in the interaction region. The trigger has an efficiency of $(97 \pm 3)\%$ for hadronic inelastic PbPb collisions. Because of hardware limits on the data acquisition rate, only a small fraction (2%) of all minimum bias events were recorded (i.e., the trigger is “prescaled”). To enhance the event sample for very central PbPb collisions, a dedicated online trigger was implemented by simultaneously requiring the HF transverse energy (E_T) sum to be greater than 3260 GeV and the pixel cluster multiplicity to be greater than 51400 (which approximately corresponds to 9500 charged particles over 5 units of pseudorapidity).

The selected events correspond to the 0.2% most central PbPb collisions. Other standard PbPb centrality classes presented in this paper are determined based on the total energy deposited in the HF calorimeters [11]. The inefficiencies of the minimum bias trigger and event selection for very peripheral events are properly taken into account.

To further reduce the background from single-beam interactions (e.g., beam-gas and beam-halo), cosmic muons, and ultra peripheral collisions that lead to the electromagnetic breakup of one or both Pb nuclei [39], offline PbPb event selection criteria [11] are applied by requiring energy deposits in at least three towers in each of the HF calorimeters, with at least 3 GeV of energy in each tower, and the presence of a reconstructed primary vertex containing at least two tracks. The reconstructed primary vertex is required to be located within ± 15 cm of the average interaction region along the beam axis and within a radius of 0.02 cm in the transverse plane. Following the procedure developed in Ref. [13], events with large signals in both Zero Degree Calorimeter (ZDC) and HF are identified as having at least one additional interaction, or pileup events, and thus rejected (about 0.1% of all events).

The reconstruction of the primary event vertex and of the trajectories of charged particles in PbPb collisions are based on signals in the silicon pixel and strip detectors and described in detail in Ref. [11]. From studies based on PbPb events simulated using HYDJET v1.8 [40], the combined geometrical acceptance and reconstruction efficiency of the primary tracks is about 70% at $p_T \sim 1$ GeV/c and $|\eta| < 1.0$ for the most central 0–5% PbPb events, but drops to about 50% for $p_T \sim 0.3$ GeV/c. The fraction of misidentified tracks is kept at the level of $< 5\%$ over most of the p_T (> 0.5 GeV/c) and $|\eta|$ (< 1.6) ranges. It increases to about 20% for very low p_T (< 0.5 GeV/c) particles in the forward ($|\eta| \geq 2$) region.

3.2 pPb data

Minimum bias pPb events were selected by requiring that at least one track with $p_T > 0.4$ GeV/c is found in the pixel tracker in coincidence with a pPb bunch crossing. About 0.1% of all minimum bias pPb events were recorded. In order to select high-multiplicity pPb collisions, a dedicated high-multiplicity trigger was implemented using the CMS level-1 (L1) and high-level trigger (HLT) systems. At L1, the total transverse energy measured using both ECAL and HCAL is required to be greater than a given threshold (20 or 40 GeV). Online track reconstruction for the HLT was based on the three layers of pixel detectors, and required a track origin within a cylindrical region, centered at the average interaction point of two beams, of length 30 cm along the beam and radius 0.2 cm perpendicular to the beam. For each event, the vertex reconstructed with the highest number of pixel tracks was selected. The number of pixel tracks ($N_{\text{trk}}^{\text{online}}$) with $|\eta| < 2.4$, $p_T > 0.4$ GeV/c, and a distance of closest approach of 0.4 cm or less to this vertex, was determined for each event.

Offline selections similar to those used for the PbPb data sample are applied to reject non-hadronic pPb interactions. A coincidence of at least one HF calorimeter tower with more than 3 GeV of total energy in each of the HF detectors is required. Events are also required to contain at least one reconstructed primary vertex within 15 cm of the nominal interaction point along the beam axis and within 0.15 cm transverse to the beam trajectory. At least two reconstructed tracks are required to be associated with the primary vertex. Beam-related background is suppressed by rejecting events for which less than 25% of all reconstructed tracks are of sufficiently good quality to be tracks selected for physics analysis, as will be discussed later in this section. Among those pPb interactions simulated with the EPOS [41] and HIJING [42] event generators that have at least one primary particle with total energy $E > 3$ GeV in both η ranges of $-5 < \eta < -3$ and $3 < \eta < 5$, the above criteria are found to select 97–98% of the events. Pileup

events are removed based on the number of tracks associated with each vertex in a bunch crossing and the distance between different vertices [22]. A purity of 99.8% for single pPb collision events is achieved for the highest multiplicity pPb interactions studied in this paper.

For the pPb analysis, the standard track reconstruction as in pp collisions is applied. The CMS high-purity tracks (as defined in Ref. [43]) are used. Additionally, a reconstructed track is only considered as a primary-track candidate if the significance of the separation along the beam axis (z) between the track and primary vertex, $d_z/\sigma(d_z)$, and the significance of the impact parameter relative to the primary vertex transverse to the beam, $d_T/\sigma(d_T)$, are each less than 3. The relative uncertainty in the transverse momentum measurement, $\sigma(p_T)/p_T$, is required to be less than 10%. To ensure high tracking efficiency and to reduce the rate of misidentified tracks, only tracks within $|\eta| < 2.4$ and with $p_T > 0.3$ GeV/ c are used in the analysis.

The entire pPb data set is divided into classes of reconstructed track multiplicity, $N_{\text{trk}}^{\text{offline}}$, where primary tracks with $|\eta| < 2.4$ and $p_T > 0.4$ GeV/ c are counted. The multiplicity classification in this analysis is identical to that used in Ref. [22], where more details are provided. The more central (0–50%) PbPb data, including ultra-central triggered events, are analyzed with a standard reconstruction algorithm used in heavy ion collisions, as described in Section 3.1. In order to compare the pPb and PbPb systems at the same collision multiplicity, peripheral PbPb events for 50–100% centrality are reprocessed using the same event selections and track reconstruction as for the pPb analysis.

4 Transverse momentum dependence of factorization breakdown

4.1 Analysis technique

The p_T -dependent factorization breaking effect is investigated using the same analysis technique of two-particle azimuthal correlations as that applied in Ref. [13]. For simplicity, a pair of two charged tracks are labeled as particle a and b (equivalent to the trigger and associated particles used in previous publications). They are selected from the same or different p_T^a and p_T^b ranges within $|\eta^{a,b}| < 2.4$. The two-particle Fourier coefficients, $V_{n\Delta}$, are calculated as the average value of $\cos(n\Delta\phi)$ over all particle pairs, which fulfill the requirement of $|\Delta\eta| > 2$ (to avoid the short-range correlations from jets and resonance decays):

$$V_{n\Delta} \equiv \langle\langle \cos(n\Delta\phi) \rangle\rangle_S - \langle\langle \cos(n\Delta\phi) \rangle\rangle_B, \quad (4)$$

in given ranges of p_T^a and p_T^b . Here, $\langle\langle \rangle\rangle$ denotes averaging over all particle pairs in each event and over all the events. The subscript S corresponds to the average over pairs taken from the same event, while B represents the mixing of particles from two randomly-selected events in the same 2 cm wide range of the primary vertex position in the z direction and from the same centrality (track multiplicity) class. The $\langle\langle \cos(n\Delta\phi) \rangle\rangle_B$ term, which is typically two orders of magnitude smaller than the corresponding S term, is subtracted to account for the effects of detector non-uniformity. This analysis is equivalent to those in Refs. [10, 22, 44, 45], where the two-particle azimuthal correlation function is first constructed and then fit with a Fourier series. The advantage of the present approach is that the extracted Fourier harmonics will not be affected by the finite bin widths of the histogram in $\Delta\eta$ and $\Delta\phi$ of the two-particle correlation function, which is relevant for higher-order Fourier harmonics.

With the $V_{n\Delta}(p_T^a, p_T^b)$ values as a function of p_T^a and p_T^b , the factorization ratio,

$$r_n(p_T^a, p_T^b) \equiv \frac{V_{n\Delta}(p_T^a, p_T^b)}{\sqrt{V_{n\Delta}(p_T^a, p_T^a)V_{n\Delta}(p_T^b, p_T^b)}}, \quad (5)$$

has been proposed as a direct measurement of the factorization breakdown effect and to explore the p_T -dependent event plane angle fluctuations in the context of hydrodynamics [23]. Here, the $V_{n\Delta}$ coefficients are calculated by pairing particles within the same p_T interval (denominator) or from different p_T intervals (numerator). If the factorization relation of Eq. (3) holds, this ratio is expected to be unity. However, with the presence of a p_T -dependent event plane angle, it can be shown that the factorization ratio, r_n , is equivalent to

$$r_n(p_T^a, p_T^b) = \frac{\langle v_n(p_T^a)v_n(p_T^b) \cos\{n[\Psi_n(p_T^a) - \Psi_n(p_T^b)]\} \rangle}{\sqrt{\langle v_n^2(p_T^a) \rangle \langle v_n^2(p_T^b) \rangle}}, \quad (6)$$

where $\Psi_n(p_T^a)$ and $\Psi_n(p_T^b)$ represent the event plane angles determined using particles from p_T^a and p_T^b intervals, respectively [23, 24], and $\langle \rangle$ denotes averaging over all the events. As one can see from Eq. (6), r_n is in general less than unity in the presence of the p_T -dependent event plane angle Ψ_n fluctuations.

4.2 Results for PbPb data

The first measurement of p_T -dependent factorization breakdown in PbPb collisions was presented in Ref. [13]. Our analysis is expanded to cover a much wider centrality range from 0% to 50%, and also includes a systematic comparison to hydrodynamic models. The values of $r_2(p_T^a, p_T^b)$ and $r_3(p_T^a, p_T^b)$ in PbPb collisions at $\sqrt{s_{\text{NN}}} = 2.76$ TeV are presented as a function of $p_T^a - p_T^b$ in Figs. 1 and 2, for several p_T^a ranges in seven different centrality classes from 0–0.2% to 40–50%. The average p_T values within each p_T^a and p_T^b range are used in order to calculate the difference between p_T^a and p_T^b . By construction, the r_n value for the highest analyzed p_T^b range, where both particles are selected from the same p_T interval, is equal to one. Only results for $p_T^a \geq p_T^b$ are presented, with a maximal p_T^a value of 3 GeV/c, a kinematic regime where the hydrodynamic flow effect is believed to be dominant. The error bars correspond to statistical uncertainties, while systematic uncertainties are found to be negligible for the r_n results (mainly because systematic uncertainties of $V_{n\Delta}$ are typically on the order of a few percent, and ratios of $V_{n\Delta}$ are taken to form r_n in this paper, where systematic uncertainties mostly cancel) and thus are not shown in any of the figures.

A clear deviation from unity of the r_2 value (Fig. 1) is observed for the highest p_T ranges in very central PbPb collisions. For each centrality class, the effect becomes more pronounced with an increase of p_T^a and also the difference between p_T^a and p_T^b values. This trend is expected as event-by-event initial-state geometry fluctuations play a more dominant role as the collisions become more central. The factorization breakdown effect reaches 20% in the ultra-central 0–0.2% events for the greatest difference between p_T^a and p_T^b . For more peripheral centrality classes, the maximum effect is a few percent. Calculations using viscous hydrodynamics [24] are performed in all centrality classes, and shown as the curves in Fig. 1. To focus on the effect of initial-state fluctuations, the η/s value is fixed at 0.12. Two different models of initial conditions, MC-Glauber [46, 47] and MC-KharzeevLevinNardi (MC-KLN; motivated by the concept of gluon saturation) [48], are compared to data. The qualitative trend of the data is consistent with hydrodynamic calculations. However, quantitatively, neither of the two models can describe all the data. The MC-Glauber model matches better the data for central collisions, while MC-KLN model appears to describe the data in the peripheral centrality range.

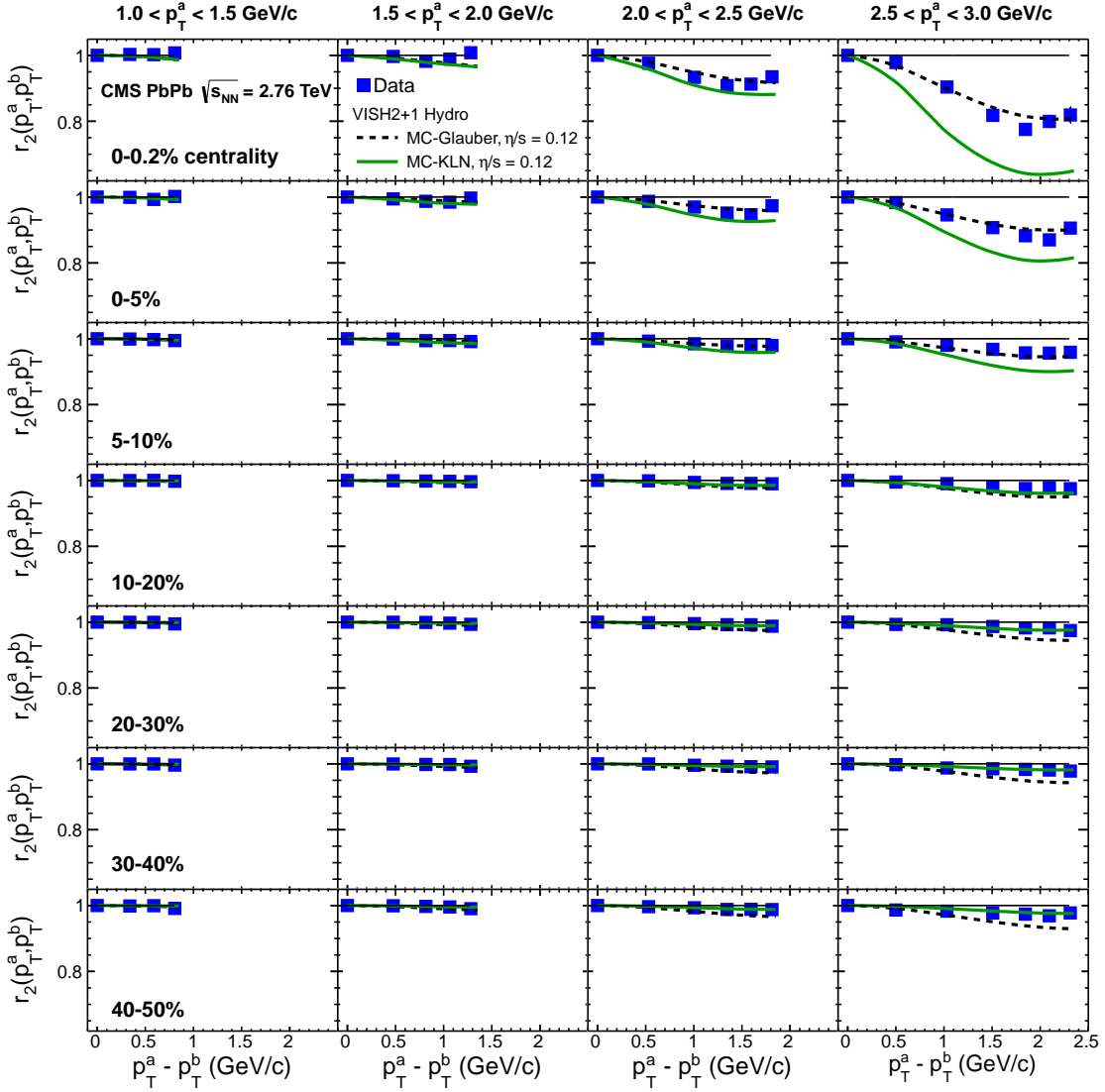


Figure 1: (Color online) The p_T -dependent factorization ratio, r_2 , as a function of $p_T^a - p_T^b$ in bins of p_T^a for different centrality ranges of PbPb collisions at $\sqrt{s_{\text{NN}}} = 2.76$ TeV. The curves show the calculations from a viscous hydrodynamic model [24] using MC-Glauber and MC-KLN initial condition models, and an η/s value of 0.12. Each row represents a different centrality range, while each column corresponds to a different p_T^a range. The horizontal solid lines denote the r_2 value of unity. The error bars correspond to statistical uncertainties, while systematic uncertainties are negligible for the r_n results, and thus are not shown.

For the third-order harmonics ($n = 3$), the effect of factorization breakdown is significantly smaller than for the second-order harmonics. Only a weak centrality dependence of r_3 is seen in Fig. 2. The biggest deviation of r_3 from unity is about 5% at large values of $p_T^a - p_T^b$ (i.e., > 1 GeV/c). Again, the qualitative features of the data are described by the hydrodynamic model, although the effects are over-estimated for peripheral collisions by the model. Calculations of r_3 using two different initial-state models yield similar results, with MC-KLN model showing a slightly stronger centrality dependence.

To understand better how the effects of factorization breakdown and p_T -dependent event plane fluctuations are influenced by the initial-state conditions and the value of η/s in hydrody-

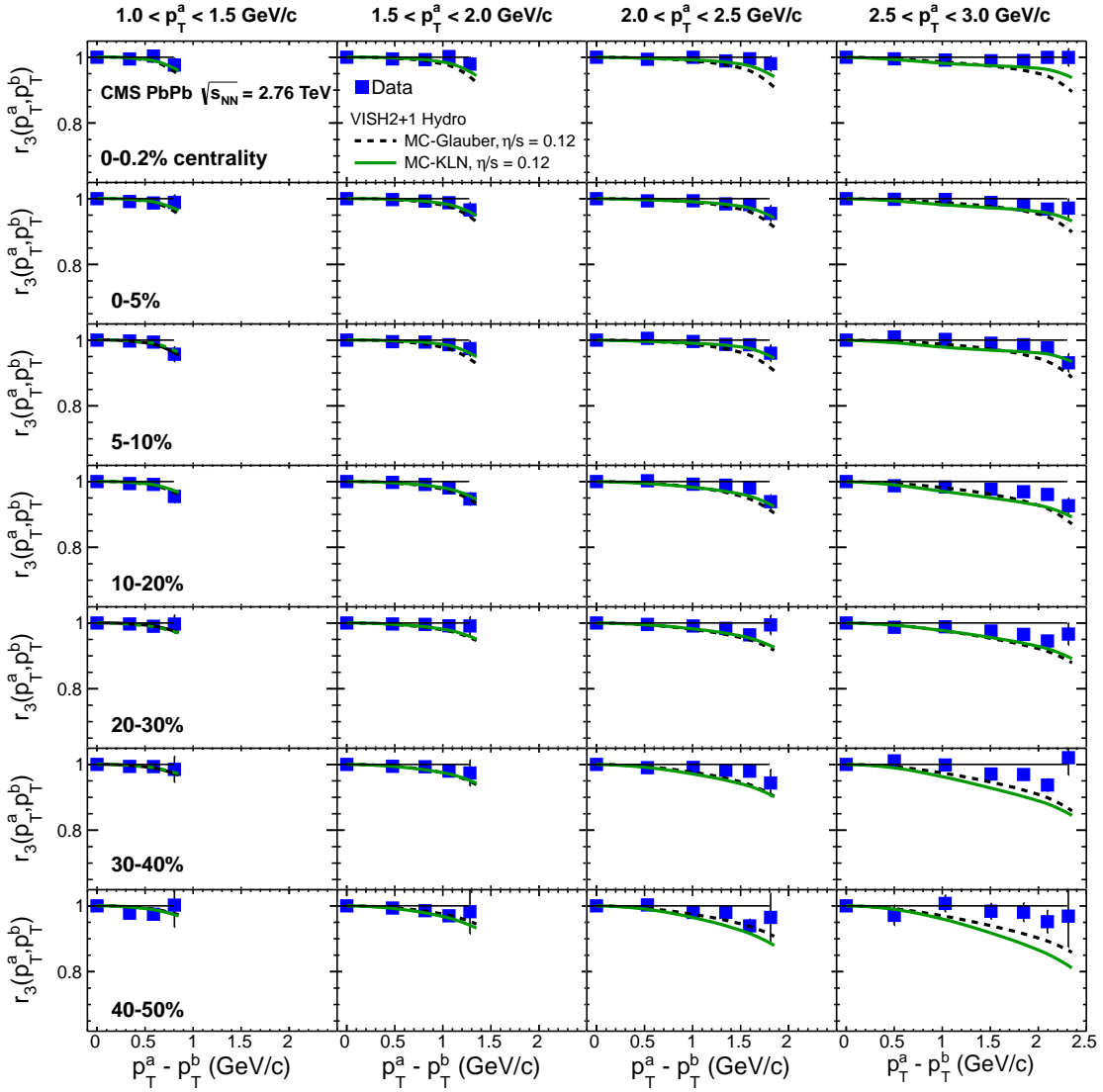


Figure 2: (Color online) Similar distributions as shown in Fig. 1, but for the factorization ratio r_3 .

dynamic models, a detailed comparison of measured r_2 values in 0–0.2% centrality PbPb collisions (where the effect is most evident) to hydrodynamic calculations is shown in Fig. 3. For this comparison, calculations with MC-Glauber and MC-KLN initial conditions are each performed for three different η/s values and compared to data. For each initial-state model, the r_2 values are found to be largely insensitive to different values of η/s . This is because, in defining $r_n(p_T^a, p_T^b)$, the magnitudes of anisotropy harmonics, which have a much greater sensitivity to η/s , are mostly canceled. Fluctuations of the event plane angle in p_T are mainly driven by the non-smooth local fluctuations in the initial energy density distribution. This comparison shows that the use of r_n data can provide new constraints on the detailed modeling of the initial-state condition and the fluctuations of the medium created in heavy ion collisions, which is independent of the η/s value. The better constraints on the initial-state conditions found using the r_n data will, in turn, improve the uncertainties of determining the medium's transport properties (e.g., η/s) using other experimental observables (e.g., the v_n magnitude, which is sensitive to both the initial state and η/s).

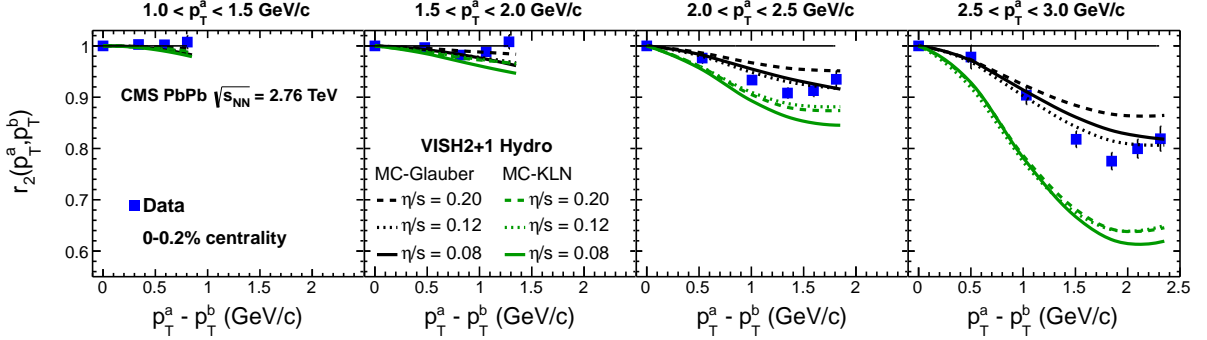


Figure 3: (Color online) Factorization ratio, r_2 , as a function of $p_T^a - p_T^b$ in bins of p_T^a for 0–0.2% centrality PbPb data at $\sqrt{s_{NN}} = 2.76$ TeV compared to viscous hydrodynamic calculations [24] using MC-Glauber and MC-KLN initial condition models, and three different values of η/s . The horizontal solid lines denote the r_2 value of unity. The error bars correspond to statistical uncertainties, while systematic uncertainties are negligible for the r_n results and thus are not shown.

4.3 Results for pPb data

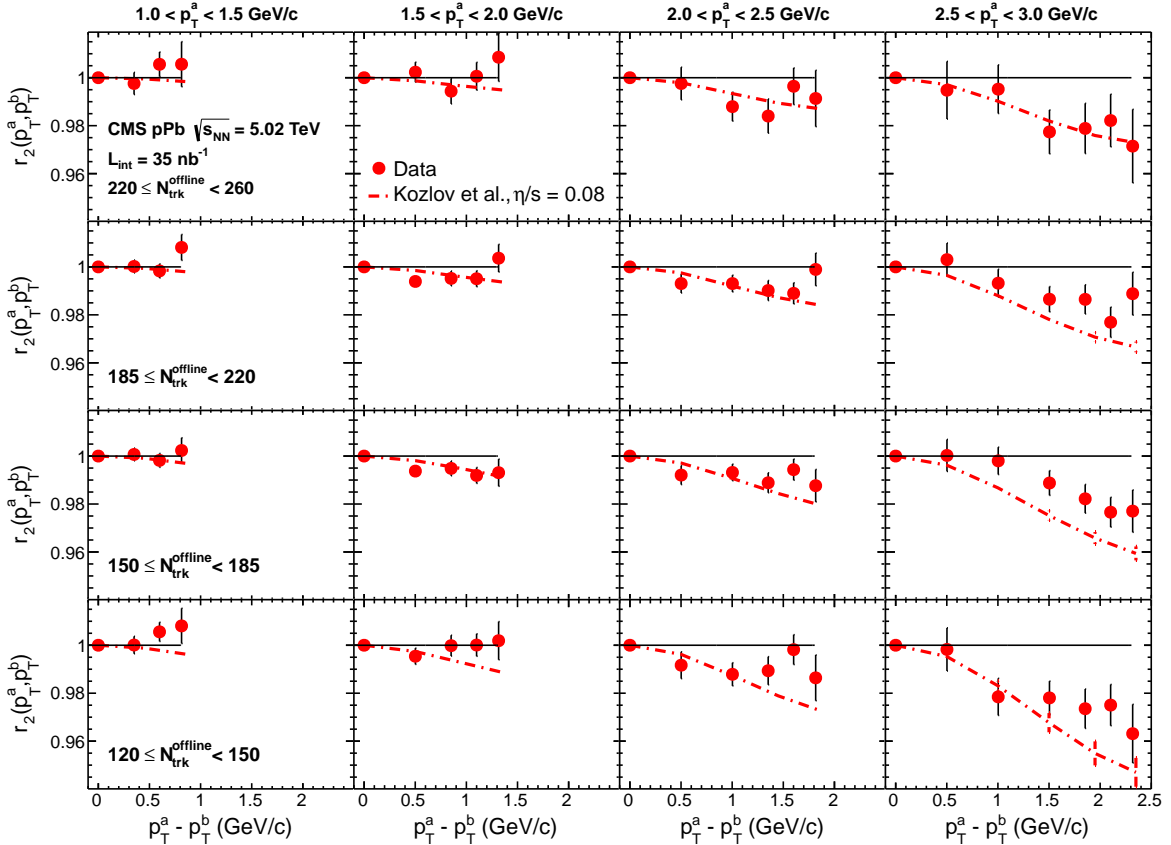


Figure 4: (Color online) The p_T -dependent factorization ratio, r_2 , as a function of $p_T^a - p_T^b$ in bins of p_T^a for four $N_{trk}^{offline}$ ranges in 5.02 TeV pPb collisions. The curves show the predictions from hydrodynamic calculations for pPb collisions of Ref. [25]. The horizontal solid lines denote the r_2 value of unity. The error bars correspond to statistical uncertainties, while systematic uncertainties are negligible for the r_n results and thus are not shown.

To gain insights into the origin of long-range correlations observed in high-multiplicity pPb

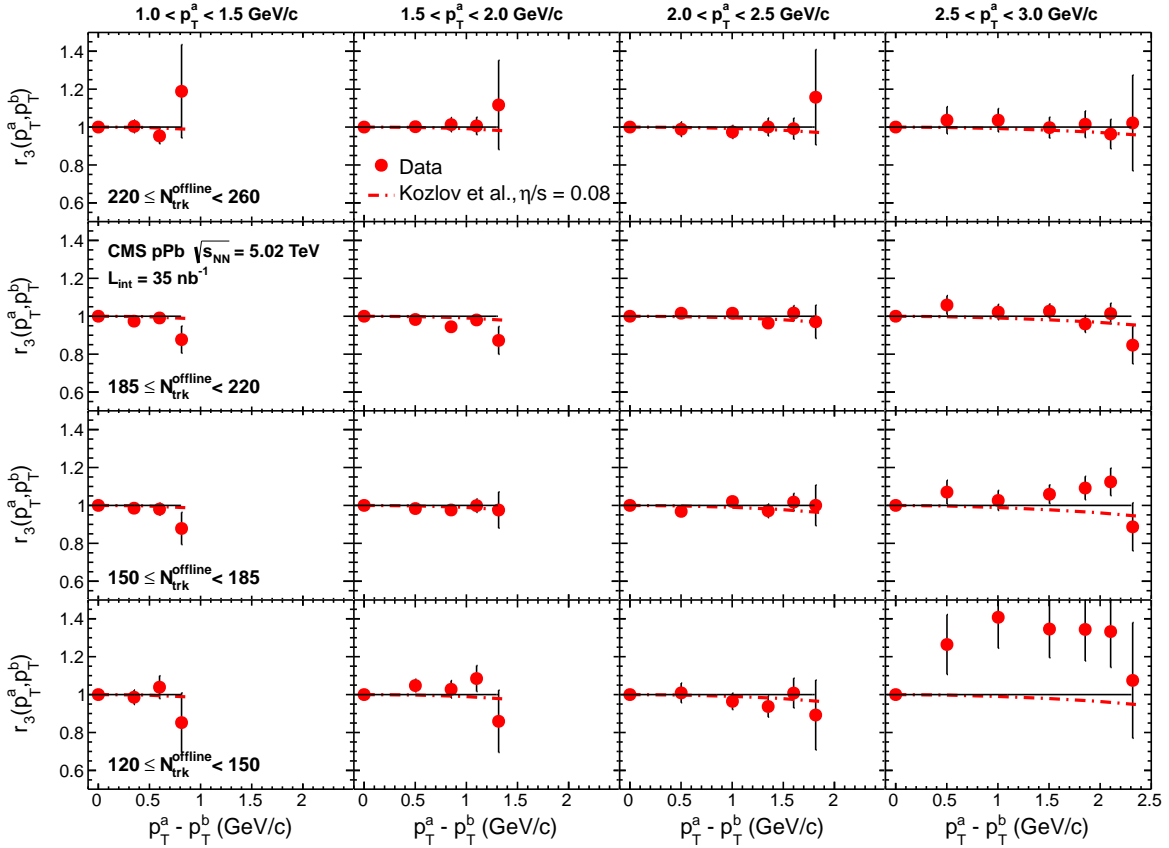


Figure 5: (Color online) Similar distributions as shown in Fig. 4, but for the factorization ratio r_3 .

collisions, the measurement of r_2 and r_3 is also performed for pPb data at $\sqrt{s_{\text{NN}}} = 5.02$ TeV for four different high-multiplicity ranges. The results are shown in Figs. 4 and 5, in the same format as those for PbPb collisions, for four p_T^a ranges (of increasing p_T from left to right panels) as a function of $p_T^a - p_T^b$.

Breakdown of factorization is observed in the r_2 results of pPb collisions for all multiplicity ranges investigated in this paper. Similar to PbPb collisions, for any multiplicity range, the effect gets larger with an increase in the difference between p_T^a and p_T^b values. However, the observed factorization breakdown reaches only up to 2–3% for the largest value of $p_T^a - p_T^b$ at $2.5 < p_T^a < 3.0$ GeV/c. This is significantly smaller than that seen in central PbPb collisions. Little multiplicity dependence of r_2 is observed in pPb collisions. Comparison of the CMS data to hydrodynamic predictions for pPb collisions in Ref. [25] is also shown. In this hydrodynamic calculation, a modified MC-Glauber initial-state model is employed for pPb collisions where the contributing entropy density of each participating nucleon in the transverse plane is distributed according to a 2D Gaussian distribution. The width of the transverse Gaussian function can be chosen to vary the transverse granularity of fluctuations, to which the r_n values are found to be most sensitive. The r_2 data are better described by calculations with a width parameter of 0.4 fm (curves in Fig. 4), while a width of 0.8 fm gives an r_n value of nearly unity (not shown) and thus underestimates the effect observed in the data. For both cases, the calculations are found to be insensitive to different η/s values, consistent with the hydrodynamic calculations used for more central PbPb collisions presented earlier.

Results of r_3 are shown in Fig. 5, presented in the same format as for r_2 . Within current statistical

precision, no evident breakdown of factorization is found in very-high-multiplicity pPb events ($185 < N_{\text{trk}}^{\text{offline}} < 260$), while the r_3 value exceeds unity for much lower-multiplicity pPb events at high p_T , particularly for $120 < N_{\text{trk}}^{\text{offline}} < 150$. This is a clear indication of significant nonflow effects as the event multiplicity decreases, because the r_n values predicted by hydrodynamic models with p_T -dependent event plane angle fluctuations would always be equal to or less than one, according to Eq. (6). One obvious possibility is back-to-back jet correlations, which would give a large negative contribution to $V_{3\Delta}$ at high p_T^a and p_T^b values in low multiplicity events [10]. This would lead to a significant reduction of the denominator of Eq. (6) and drives the r_3 value up above unity. Very little effect of factorization breakdown for $n = 3$ is predicted in Ref. [25], which is consistent with the data except for the low-multiplicity ranges.

4.4 Comparison of pPb and PbPb data

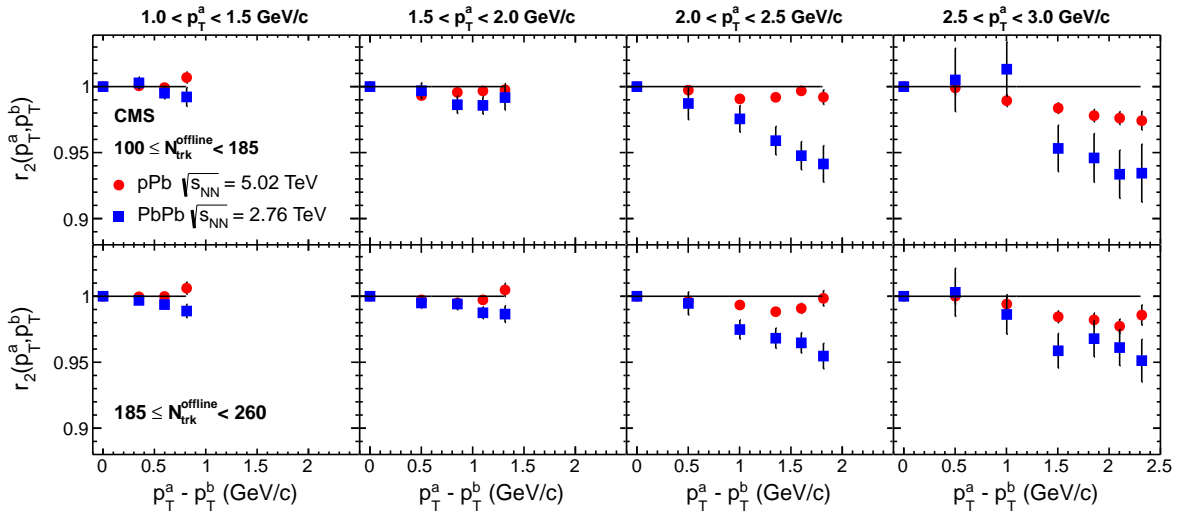


Figure 6: (Color online) The p_T -dependent factorization ratio, r_2 , as a function of $p_T^a - p_T^b$ in bins of p_T^a for two $N_{\text{trk}}^{\text{offline}}$ ranges of 5.02 TeV pPb and 2.76 TeV PbPb collisions. The horizontal solid lines denote the r_2 value of unity. The error bars correspond to statistical uncertainties, while systematic uncertainties are negligible for the r_n results and thus are not shown.

Figure 6 shows a comparison between 5.02 TeV pPb and 2.76 TeV peripheral PbPb collisions over the same multiplicity ranges. Because of the statistical limitation of the PbPb data, the multiplicity ranges used in Figs. 4 and 5 for pPb data are combined into two $N_{\text{trk}}^{\text{offline}}$ classes, $100 \leq N_{\text{trk}}^{\text{offline}} < 185$ (top) and $185 \leq N_{\text{trk}}^{\text{offline}} < 260$ (bottom). At a similar $N_{\text{trk}}^{\text{offline}}$ range, the magnitudes of factorization breakdown in pPb and PbPb collisions depart from unity by less than 8%, with slightly smaller deviations for pPb data, although the statistical precision is limited. For both high-multiplicity pPb and peripheral PbPb collisions, the observed effect is significantly smaller than that for 0–0.2% centrality ultra-central PbPb collisions (up to 20% away from unity). The similar behavior (e.g., p_T -dependence) of factorization data in pPb to that in PbPb collisions may provide new insight into the possible hydrodynamic flow origin of long-range two-particle correlations in the pPb system, particularly in providing new information on the nature of initial-state fluctuations in a much smaller volume.

To study directly the multiplicity dependence of the effect in PbPb and pPb collisions, the r_2 and r_3 results for $2.5 < p_T^a < 3.0$ GeV/c and $0.3 < p_T^b < 0.5$ GeV/c (where the difference between p_T^a and p_T^b is the greatest, $p_T^a - p_T^b \approx 2$ GeV/c) are shown in Fig. 7, as a function of event multiplicity in pPb and PbPb collisions. Here, the number of tracks is still counted with $|\eta| < 2.4$ and $p_T > 0.4$ GeV/c but corrected for the detector inefficiency, since a different track recon-

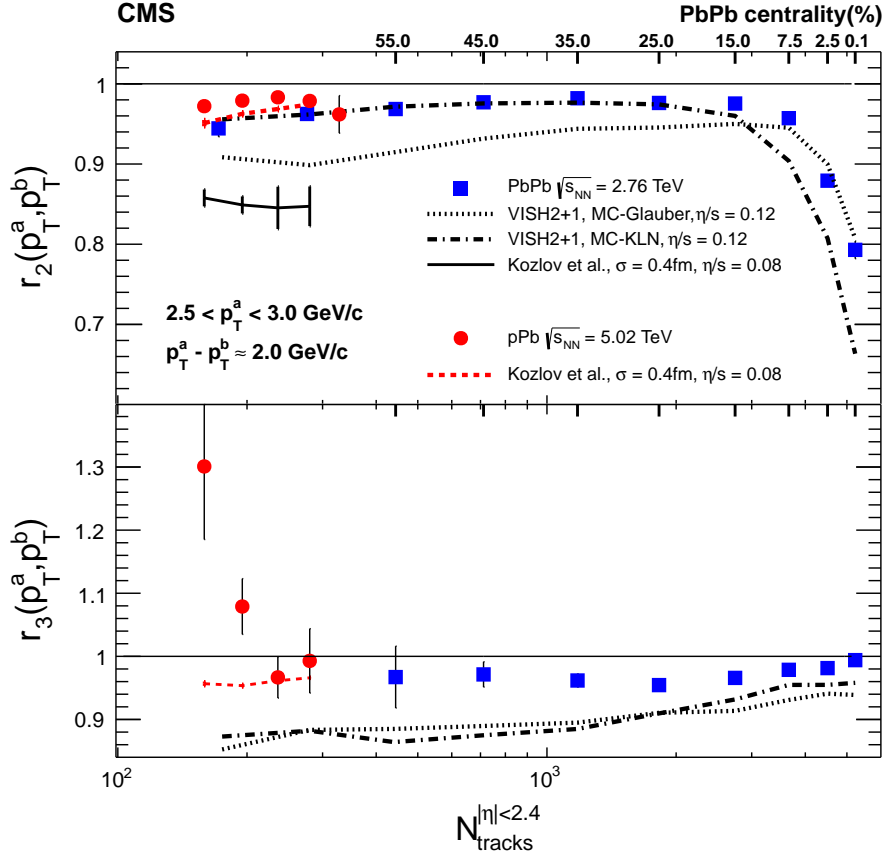


Figure 7: (Color online) The p_T -dependent factorization ratios, r_2 and r_3 , as a function of event multiplicity in pPb and PbPb collisions. The curves show the calculations for PbPb collisions from viscous hydrodynamics in Ref. [24] with MC-Glauber and MC-KLN initial condition models and $\eta/s = 0.12$, and also hydrodynamic predictions for PbPb and pPb data in Ref. [25]. The horizontal solid lines denote the r_2 (top) and r_3 (bottom) value of unity. The error bars correspond to statistical uncertainties, while systematic uncertainties are negligible for the r_n results and thus are not shown.

struction algorithm is used for the pPb and central PbPb data. Additionally, at the top of the figure, a centrality axis is shown which is applicable only to PbPb collisions. The breakdown of factorization for r_2 in PbPb events increases dramatically as the collisions become more central than 0–5%, while the effect in r_3 remains at the 2–3% level, largely independent of centrality. For more peripheral PbPb events from 20% to 80% centrality, the deviation of r_2 from unity increases slightly from about 2 to 5%. Calculations using a hydrodynamic model in PbPb collisions [24] with MC-Glauber and MC-KLN initial conditions and $\eta/s = 0.12$ are also shown as dotted and dash-dotted curves, respectively, as a function of centrality. As pointed out earlier, neither of the two calculations can describe the data quantitatively over the entire centrality range, although the qualitative trend is reproduced. The r_2 values for pPb show little multiplicity dependence, consistent with hydrodynamic predictions in Ref. [25]. The r_3 values for pPb go significantly above unity at lower multiplicities, because of the onset of nonflow correlations. The discrepancy in the hydrodynamic calculations of r_2 for peripheral PbPb collisions between Ref. [24] and Ref. [25] may be related to differences in some model parameters (e.g., transverse size of the nucleon). This should be investigated in the future.

Although the factorization results presented in this paper suggest a breakdown of the assump-

tion commonly applied in studying collective flow using two-particle correlations (Eq. (3)), previous v_n measurements from the two-particle method still remain valid. However, they should be more precisely interpreted as the v_n values obtained with respect to an averaged event plane using particles from a given kinematic regime (usually over a wide p_T range). The studies in this paper also point out the importance of applying the same conditions for theoretical calculations when comparing to the experimental data.

5 Pseudorapidity dependence of factorization breakdown

5.1 Analysis technique

In principle, the η -dependent factorization breakdown and event plane angle fluctuations can be examined using a similar formalism to Eq. (5) by replacing p_T^a and p_T^b with η^a and η^b . However, the main issue with this approach is that the requirement of $|\Delta\eta| > 2$ for removing short-range two-particle correlations cannot be fulfilled anymore as the denominator of the factorization ratio takes the $V_{n\Delta}(\eta^a, \eta^b)$ components, where $\eta^a \approx \eta^b$. The correlation signal from collective flow is strongly contaminated by short-range jet-like correlations. To avoid this problem, an alternative observable is developed for the study of η -dependent factorization, by taking advantage of the wide η coverage of the CMS tracker and HF calorimeters.

The η -dependent factorization ratio, $r_n(\eta^a, \eta^b)$, is defined as

$$r_n(\eta^a, \eta^b) \equiv \frac{V_{n\Delta}(-\eta^a, \eta^b)}{V_{n\Delta}(\eta^a, \eta^b)}, \quad (7)$$

where $V_{n\Delta}(\eta^a, \eta^b)$ is calculated in the same way as Eq. (4) but for pairs of particles taken from varied η^a and η^b regions in fixed p_T^a and p_T^b ranges. Here, particle a is chosen from charged tracks with $0.3 < p_T^a < 3.0 \text{ GeV}/c$ and $|\eta^a| < 2.4$, while particle b is selected from the HF calorimeter towers with the energy exceeding 1 GeV (with a total coverage of $2.9 < |\eta| < 5.2$) without any explicit transverse energy (E_T) threshold for each tower. With this approach, the η values of both particles from a pair can be varied over a wide range, while it is possible to ensure a large η gap by combining detector components covering central and forward η regions. As illustrated by a schematic in Fig. 8, for $4.4 < \eta^b < 5.0$ from the HF calorimeters, a minimum η gap of 2 units between a calorimeter tower and any charged particle from the silicon tracker is guaranteed. Away-side back-to-back jet correlations could still be present but they are shown to have a negligible contribution at low p_T because of very high multiplicities [22], especially in central PbPb collisions. To account for any occupancy effect of the HF detectors due to large granularities in η and ϕ , each tower is weighted by its E_T value when calculating the average in Eq. (4). For consistency, each track is also weighted by its p_T value. The finite azimuthal resolution of the HF towers (0.349 radians) has negligible effects to the $V_{n\Delta}$ calculation, which takes an E_T -weighted average of 36 tower segments over a 2π coverage.

If, for each event, the event plane angle, Ψ_n , does vary for particles produced at different η regions, the following relation for $r_n(\eta^a, \eta^b)$ can be derived,

$$r_n(\eta^a, \eta^b) = \frac{\langle v_n(-\eta^a)v_n(\eta^b) \cos\{n[\Psi_n(-\eta^a) - \Psi_n(\eta^b)]\} \rangle}{\langle v_n(\eta^a)v_n(\eta^b) \cos\{n[\Psi_n(\eta^a) - \Psi_n(\eta^b)]\} \rangle}. \quad (8)$$

In symmetric collision systems like PbPb, v_n harmonics from symmetric positive ($v_n(\eta^a)$) and negative ($v_n(-\eta^a)$) η regions are identical after averaging over all events. Therefore, Eq. (8) can

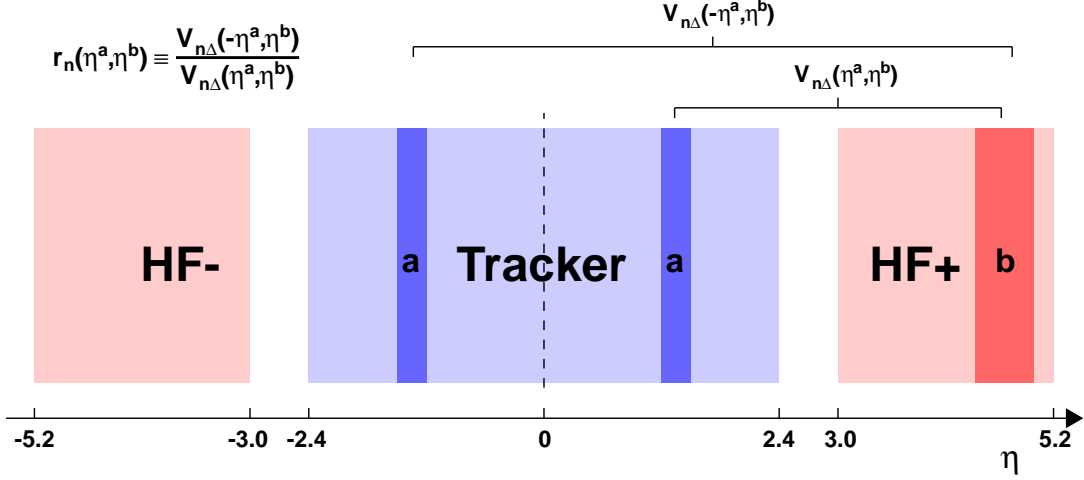


Figure 8: (Color online) A schematic illustrating the acceptance coverage of the CMS tracker and HF calorimeters, and the procedure for deriving the η -dependent factorization ratio, $r_n(\eta^a, \eta^b)$.

be approximated by

$$r_n(\eta^a, \eta^b) \approx \frac{\langle \cos [n (\Psi_n(-\eta^a) - \Psi_n(\eta^b))] \rangle}{\langle \cos [n (\Psi_n(\eta^a) - \Psi_n(\eta^b))] \rangle}. \quad (9)$$

Here, the approximation is due to the fact that the flow magnitude (v_n) and the orientation angle (Ψ_n) are inside the same averaging over all the events in the numerator of Eq. (8). As a result, $r_n(\eta^a, \eta^b)$ represents a measurement of relative event plane angle fluctuations in η for planes separated by $|\eta^a + \eta^b|$ and $|\eta^a - \eta^b|$. Similar to $r_n(p_T^a, p_T^b)$, $r_n(\eta^a, \eta^b)$ is equal to unity if the factorization holds but factorization breaks down in general in the presence of event plane fluctuations in η .

For an asymmetric collision system like pPb, $v_n(\eta^a)$ and $v_n(-\eta^a)$ are not identical in general, and thus η -dependent event plane fluctuation effect cannot be isolated in Eq. (8). However, by taking a product of $r_n(\eta^a, \eta^b)$ and $r_n(-\eta^a, -\eta^b)$, the v_n terms can be removed,

$$\sqrt{r_n(\eta^a, \eta^b)r_n(-\eta^a, -\eta^b)} \approx \sqrt{\frac{\langle \cos [n (\Psi_n(-\eta^a) - \Psi_n(\eta^b))] \rangle}{\langle \cos [n (\Psi_n(\eta^a) - \Psi_n(\eta^b))] \rangle} \frac{\langle \cos [n (\Psi_n(\eta^a) - \Psi_n(-\eta^b))] \rangle}{\langle \cos [n (\Psi_n(-\eta^a) - \Psi_n(-\eta^b))] \rangle}}. \quad (10)$$

In this way, the η -dependent event plane angle fluctuations in pPb collisions can also be studied.

5.2 Results for PbPb data

The results of η -dependent factorization ratios, r_2 , r_3 and r_4 in PbPb collisions at $\sqrt{s_{\text{NN}}} = 2.76$ TeV are shown in Figs. 9–11, as a function of η^a for eight different centrality classes from 0–0.2% to 50–60% (except for r_4 , for which only three centrality classes are shown because of statistical limitations). The $r_2(\eta^a, \eta^b)$ values are calculated in η^a bins of 0.3 units, and the η^a value at the center of each bin is used in the plots. Data obtained with calorimeter tower η ranges $3.0 < \eta^b < 4.0$ and $4.4 < \eta^b < 5.0$ are both presented. Since PbPb is a symmetric system, the $V_n(\eta^a, \eta^b)$ and $V_n(-\eta^a, -\eta^b)$ coefficients are combined before calculating the r_n ratios in order to achieve the optimal statistical precision. Charged tracks within $0.3 < p_T < 3.0$ GeV/c and all calorimeter towers ($E > 1$ GeV) are used. When $\eta^a = 0$, the r_n value is equal to unity by construction since both the numerator and denominator of r_n have the same η gap between

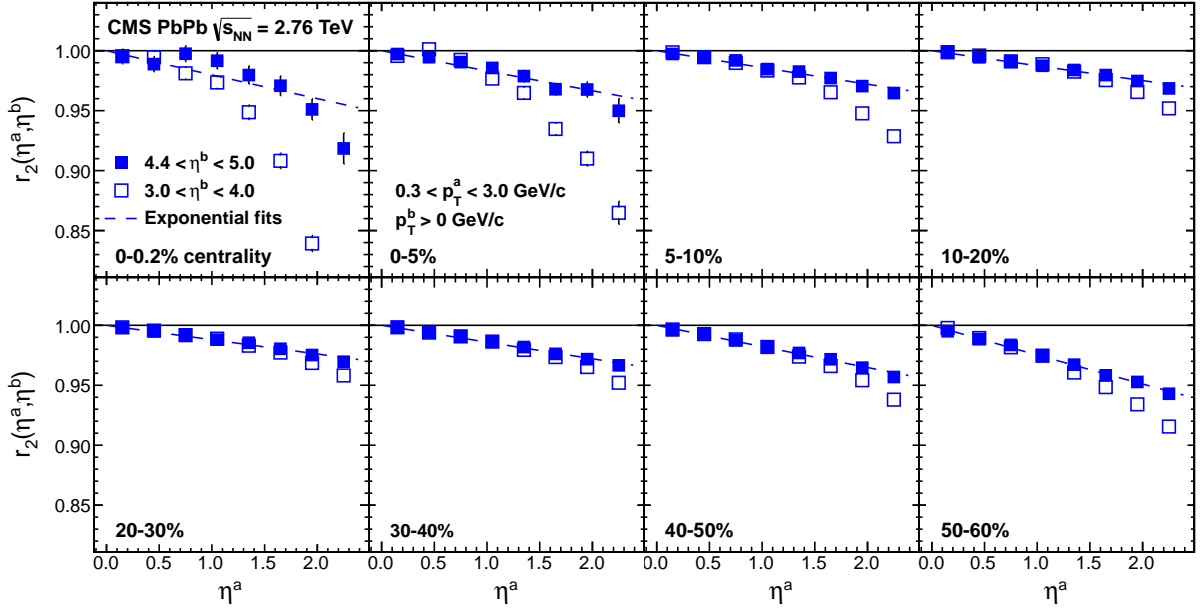


Figure 9: (Color online) The η -dependent factorization ratio, r_2 , as a function of η^a for $3.0 < \eta^b < 4.0$ and $4.4 < \eta^b < 5.0$, averaged over $0.3 < p_T^a < 3.0$ GeV/c, in eight centrality classes of PbPb collisions at $\sqrt{s_{NN}} = 2.76$ TeV. The curves correspond to fits to the data for $4.4 < \eta^b < 5.0$ given by Eq. (12). The horizontal solid lines denote the r_2 value of unity. The error bars correspond to statistical uncertainties, while systematic uncertainties are negligible for the r_n results, and thus are not shown.

particle a and b , as indicated in Eq. (9). As η^a increases, a significant decrease of r_n below unity is observed, which may suggest the presence of η -dependent event plane angle fluctuations.

The r_2 values for $4.4 < \eta^b < 5.0$ are found to decrease with η^a approximately linearly for most of the centrality classes up to a few percent deviation below unity at $\eta^a \sim 2.4$. This behavior is slightly different for the most central 0–0.2% events, where the decrease of r_2 becomes more significant at $\eta^a \sim 1$. For $3.0 < \eta^b < 4.0$, the r_2 value exhibits a much stronger factorization breakdown effect for an $\eta^a > 1$. This can be understood as the effect of short-range jet-like correlations when the η gap between two particles is less than 2, which increases the denominator of Eq. (7). However, for $\eta^a < 1$, the r_2 results are found to be consistent with each other, independent of η^b (except for 0–0.2% centrality). This demonstrates that contributions of short-range jet-like correlations are almost completely suppressed if the requirement of $|\Delta\eta| > 2$ to both numerator and denominator of $r_n(\eta^a, \eta^b)$ is imposed.

The effect of η -dependent factorization breakdown is much stronger for higher-order harmonics, r_3 and r_4 , shown in Figs. 10 and 11. For r_3 , this trend is opposite to what is observed for the p_T -dependent factorization ratio. For all centrality ranges (including 0–0.2%), an approximate linear dependence of r_3 and r_4 is seen. Results from the two different η^b ranges agree over most of the η^a range within statistical uncertainties. This might suggest that short-range jet-like correlations have much smaller effects on higher-order harmonics.

As observed in Figs. 9–11, the $r_n(\eta^a, \eta^b)$ values are independent of η^b , for η^a ranges where contributions of only long-range ($|\Delta\eta| > 2$) correlations are included. To quantify the dependence of r_n values on η^a , a simple empirical parameterization is introduced:

$$\cos \left[n \left(\Psi_n(\eta^a) - \Psi_n(\eta^b) \right) \right] = e^{-F_n^{\eta} |\eta^a - \eta^b|}, \quad (11)$$

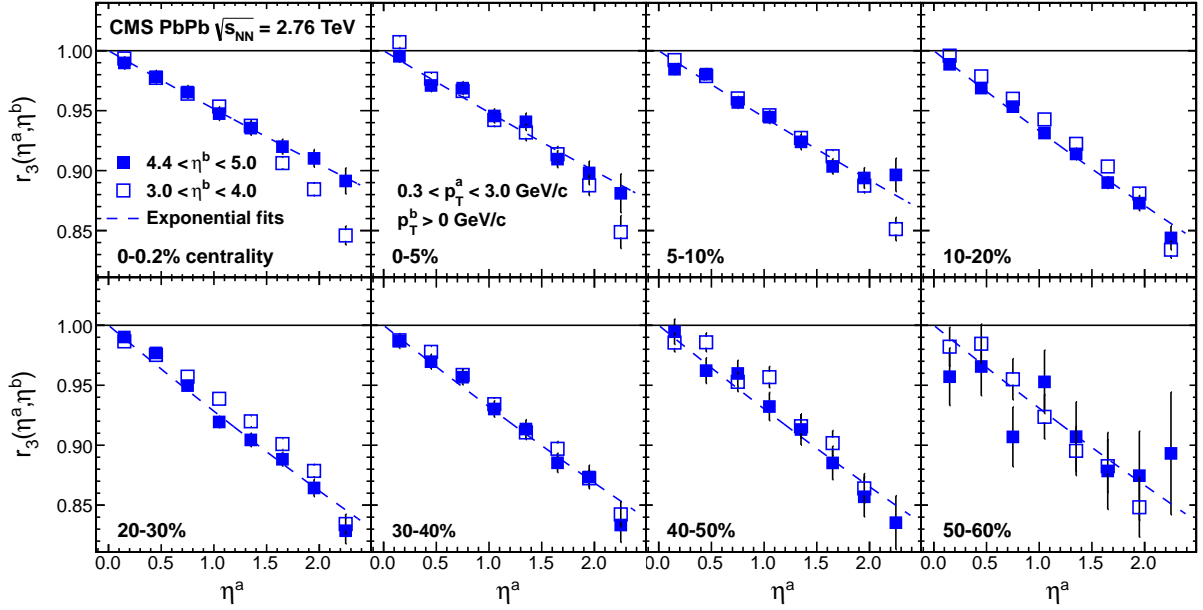


Figure 10: (Color online) Similar distributions as shown in Fig. 9, but for the factorization ratio r_3 .

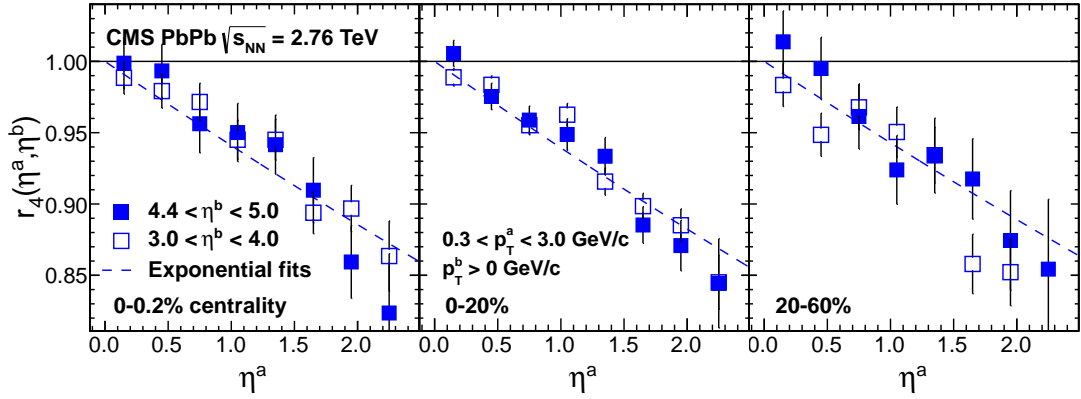


Figure 11: (Color online) Similar distributions as shown in Fig. 9, but for the factorization ratio r_4 in fewer centrality ranges.

which is based on the assumption that relative fluctuations between two event plane angles depend only on their pseudorapidity difference. At small $\Delta\eta$ values, the exponential function form can be approximated by a linear function of $\Delta\eta$, consistent with the observation in the data. By plugging Eq. (11) into Eq. (9), the r_n can be expressed as

$$r_n(\eta^a, \eta^b) \approx e^{-2F_n^{\eta^a}}, \quad (12)$$

which is independent of η^b , consistent with the results in Figs. 9–11. According to Eqs. (11) and (12), the $r_n(\eta^a, \eta^b)$ also corresponds to a measurement of event plane fluctuations between $\Psi_n(\eta^a)$ and $\Psi_n(-\eta^a)$,

$$r_n(\eta^a, \eta^b) \approx \langle \cos [n (\Psi_n(-\eta^a) - \Psi_n(\eta^a))] \rangle. \quad (13)$$

The r_2 data for $4.4 < \eta^b < 5.0$ are well fit with a functional form given by Eq. (12) for most centrality classes ($\chi^2/(\text{degree of freedom}) \sim 1$), except for 0–0.2% centrality, where the r_2 value

deviates from unity much faster as η^a increases. Note that the parameter, F_n^η , is purely empirical, without any clear physical meaning at present. It is introduced mainly for quantitatively evaluating the centrality evolution of factorization breakdown effect, as will be discussed later in Section 5.4.

5.3 Results for pPb data

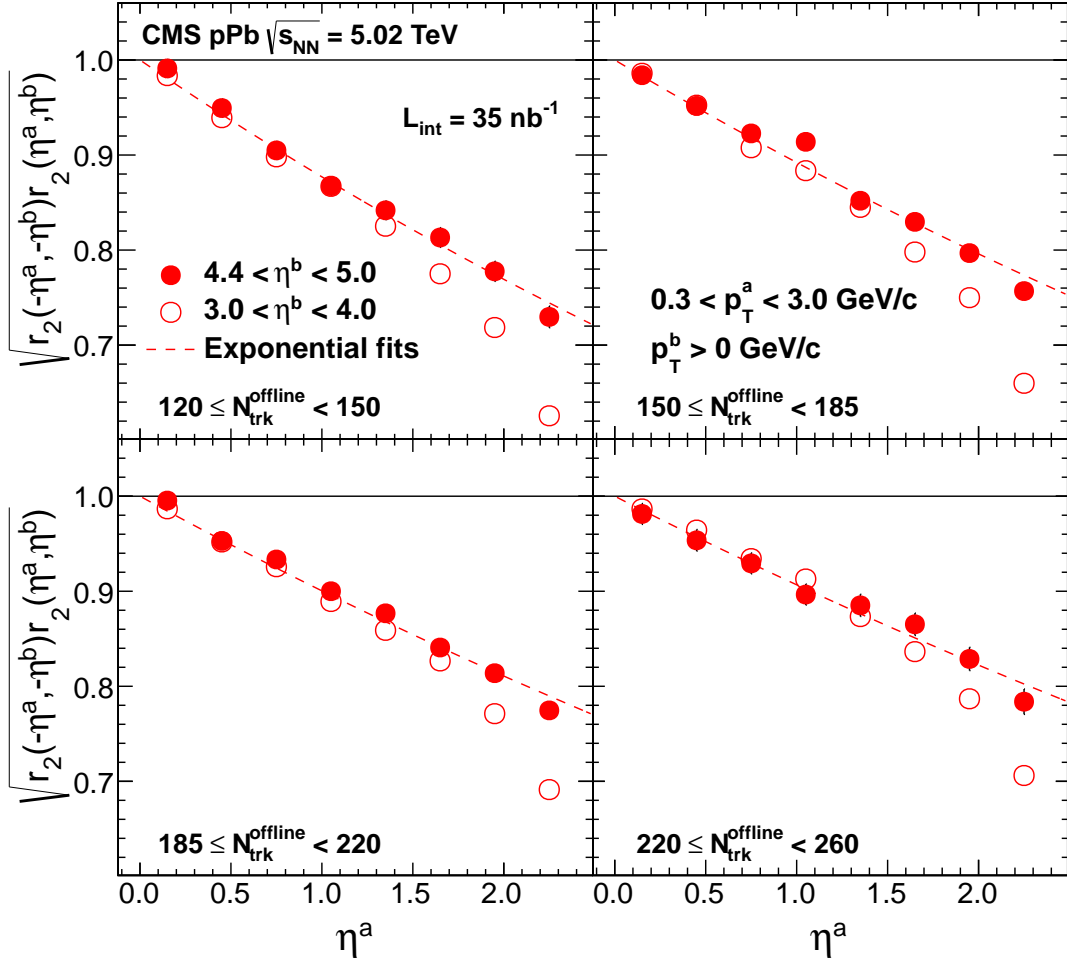


Figure 12: (Color online) The square root of the product of factorization ratios, $\sqrt{r_2(\eta^a, \eta^b)r_2(-\eta^a, -\eta^b)}$, as a function of η^a for $3.0 < \eta^b < 4.0$ and $4.4 < \eta^b < 5.0$, averaged over $0.3 < p_T^a < 3.0 \text{ GeV}/c$, in four multiplicity classes of pPb collisions at $\sqrt{s_{\text{NN}}} = 5.02 \text{ TeV}$. The curves correspond to the fits to the data for $4.4 < \eta^b < 5.0$ using Eq. (12). The horizontal solid lines denote the r_2 value of unity. The error bars correspond to statistical uncertainties, while systematic uncertainties are negligible for the r_2 results, and thus are not shown.

Studies of η -dependent factorization breakdown of two-particle correlations are also performed in pPb collisions at $\sqrt{s_{\text{NN}}} = 5.02 \text{ TeV}$ for four high-multiplicity ranges, shown in Fig. 12 for the second-order harmonics. Results for higher-order harmonics in pPb cannot be obtained due to statistical limitation. As pointed out in Section 5.1, because of asymmetry of pPb collisions in η , the factorization ratio, $r_n(\eta^a, \eta^b)$, is sensitive to asymmetry in the magnitude of v_n , and thus does not only reflect the effect of event plane angle fluctuations. Therefore, the results are presented as the square root of the product of $r_n(\eta^a, \eta^b)$ and $r_n(-\eta^a, -\eta^b)$, which is designed to remove the sensitivity to the magnitude of v_n (see Eq. (10) for details). Similar to those in

PbPb collisions, two different η ranges of HF towers, $3.0 < \eta^b < 4.0$ and $4.4 < \eta^b < 5.0$, are compared.

A significant breakdown of factorization in η is also observed in pPb collisions as η^a increases. Similar to the PbPb results, the factorization breakdown is approximately independent of η^b for $\eta^a < 1$ for all multiplicity ranges but shows a much larger deviation from unity for $3.0 < \eta^b < 4.0$ as η^a increases beyond one unit because of short-range correlations. The fits to the data for $4.4 < \eta^b < 5.0$ using Eq. (12) are also shown; the data are well-described over the accessible η^a range. It should be noted that the assumption made in Eq. (11) is purely an empirical parameterization for quantifying the behavior of the data. Since pPb collisions are asymmetric, this assumption could be invalid. More detailed investigations on how r_n depends on η^a and η^b in the proton- and lead-going directions, respectively, are needed in future work.

5.4 Comparison of pPb and PbPb data

The extracted F_n^{η} parameters are plotted as a function of event multiplicity in Fig. 13, in pPb collisions for $n = 2$ and PbPb collisions for $n = 2-4$. The F_2^{η} value reaches its minimum around midcentral ($\sim 20\%$) PbPb events, and increases significantly for more peripheral PbPb events and also for pPb events, where the relative fluctuations of v_2 are larger [12]. Toward the most central PbPb events, the F_2^{η} value also shows a tendency to increase slightly, although the r_n data for 0–0.2% centrality are not well described by Eq. (12). At a similar multiplicity, magnitudes of the F_2^{η} parameter in pPb are significantly larger than those in PbPb, and decrease with increasing event multiplicity. In PbPb collisions, a much stronger η -dependent factorization breakdown is seen for higher-order harmonics than for the second order, as shown by the F_3^{η} and F_4^{η} parameters. There is little centrality dependence for $n = 3$, except for the most central 0–20% PbPb collisions. Within current statistical uncertainties, no centrality dependence is observed for $n = 4$.

6 Summary

Factorization of azimuthal two-particle correlations into single-particle anisotropies has been studied as a function of transverse momentum and pseudorapidity of each particle from a pair, in PbPb collisions at $\sqrt{s_{\text{NN}}} = 2.76$ TeV and pPb collisions at $\sqrt{s_{\text{NN}}} = 5.02$ TeV, over a wide multiplicity range. The factorization assumption is found to be broken as a function of both p_T and η . The effect of p_T dependent factorization breakdown for the second-order Fourier harmonic is found to increase with the difference in p_T between the two particles. The factorization breakdown reaches 20% for the most central PbPb collisions, while it decreases rapidly for more peripheral collisions. The effect is significantly smaller (2–3%) in high-multiplicity pPb collisions. In both PbPb and pPb samples over the full centrality or multiplicity range, little effect is observed for the third order harmonic. For the η dependence, the observed factorization breakdown shows an approximately linear increase with the η gap between two particles for all centrality and multiplicity classes in PbPb and pPb collisions. The effect is weakest for mid-central PbPb events, but becomes larger for more central or peripheral PbPb collisions, and also for very high-multiplicity pPb collisions. Moreover, a much stronger η -dependent effect is seen for the third- and fourth-order harmonics than the second-order harmonics in PbPb collisions. This relation between the second and third order is opposite to that seen in the p_T -dependent factorization studies. The observed factorization breakdown presented here does not invalidate previous v_n measurements. Instead, the previous values should be reinterpreted as measuring anisotropies with respect to the event plane averaged over a given kinematic region. Furthermore, it is important to compare data and theoretical calculations following exactly the same

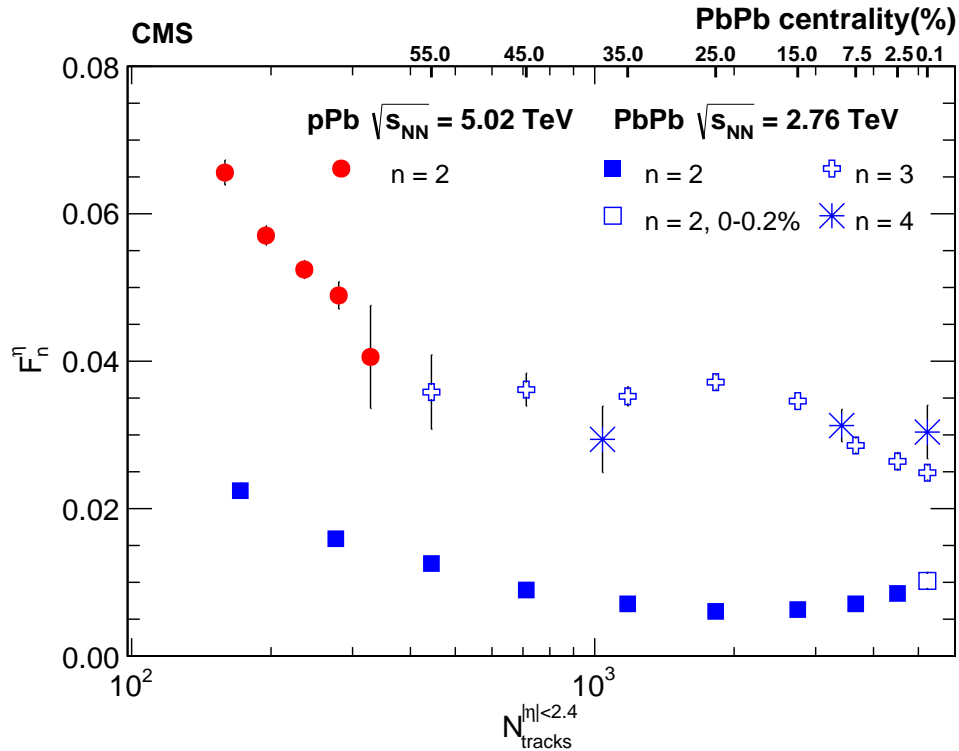


Figure 13: (Color online) The F_n^η parameter as defined in Eq. (12) as a function of event multiplicity in PbPb collisions at $\sqrt{s_{\text{NN}}} = 2.76$ TeV for $n = 2-4$ and pPb collisions at $\sqrt{s_{\text{NN}}} = 5.02$ TeV for $n = 2$. The error bars correspond to statistical uncertainties, while systematic uncertainties are negligible for the r_n results, and thus are not shown.

procedure.

The factorization data have been compared to hydrodynamic calculations with fluctuating initial-state conditions. The p_T -dependent factorization data are qualitatively described by viscous hydrodynamic models, which are shown to be largely insensitive to the value of shear viscosity to entropy density ratio of the medium. This observation offers great promise for using the factorization data to disentangle contributions of the initial-state conditions and the medium's transport properties to the observed collective flow phenomena in the final state. The new studies of η -dependent factorization breakdown give an indication of initial-state fluctuations along the longitudinal direction. This will provide new insights into the longitudinal dynamics of relativistic heavy ion collisions, and help improve the three-dimensional modeling of the evolution of the strongly-coupled quark gluon medium.

Acknowledgments

We congratulate our colleagues in the CERN accelerator departments for the excellent performance of the LHC and thank the technical and administrative staffs at CERN and at other CMS institutes for their contributions to the success of the CMS effort. In addition, we gratefully acknowledge the computing centers and personnel of the Worldwide LHC Computing Grid for delivering so effectively the computing infrastructure essential to our analyses. Finally, we acknowledge the enduring support for the construction and operation of the LHC and the CMS detector provided by the following funding agencies: BMWFW and FWF (Austria); FNRS and

FWO (Belgium); CNPq, CAPES, FAPERJ, and FAPESP (Brazil); MES (Bulgaria); CERN; CAS, MoST, and NSFC (China); COLCIENCIAS (Colombia); MSES and CSF (Croatia); RPF (Cyprus); MoER, ERC IUT and ERDF (Estonia); Academy of Finland, MEC, and HIP (Finland); CEA and CNRS/IN2P3 (France); BMBF, DFG, and HGF (Germany); GSRT (Greece); OTKA and NIH (Hungary); DAE and DST (India); IPM (Iran); SFI (Ireland); INFN (Italy); MSIP and NRF (Republic of Korea); LAS (Lithuania); MOE and UM (Malaysia); CINVESTAV, CONACYT, SEP, and UASLP-FAI (Mexico); MBIE (New Zealand); PAEC (Pakistan); MSHE and NSC (Poland); FCT (Portugal); JINR (Dubna); MON, RosAtom, RAS and RFBR (Russia); MESTD (Serbia); SEIDI and CPAN (Spain); Swiss Funding Agencies (Switzerland); MST (Taipei); ThEPCenter, IPST, STAR and NSTDA (Thailand); TUBITAK and TAEK (Turkey); NASU and SFFR (Ukraine); STFC (United Kingdom); DOE and NSF (USA).

Individuals have received support from the Marie-Curie program and the European Research Council and EPLANET (European Union); the Leventis Foundation; the A. P. Sloan Foundation; the Alexander von Humboldt Foundation; the Belgian Federal Science Policy Office; the Fonds pour la Formation à la Recherche dans l'Industrie et dans l'Agriculture (FRIA-Belgium); the Agentschap voor Innovatie door Wetenschap en Technologie (IWT-Belgium); the Ministry of Education, Youth and Sports (MEYS) of the Czech Republic; the Council of Science and Industrial Research, India; the HOMING PLUS program of the Foundation for Polish Science, cofinanced from European Union, Regional Development Fund; the Compagnia di San Paolo (Torino); the Consorzio per la Fisica (Trieste); MIUR project 20108T4XTM (Italy); the Thalís and Aristeia programs cofinanced by EU-ESF and the Greek NSRF; and the National Priorities Research Program by Qatar National Research Fund.

References

- [1] BRAHMS Collaboration, "Quark gluon plasma and color glass condensate at RHIC? The perspective from the BRAHMS experiment", *Nucl. Phys. A* **757** (2005) 1, doi:10.1016/j.nuclphysa.2005.02.130, arXiv:nucl-ex/0410020.
- [2] PHOBOS Collaboration, "The PHOBOS perspective on discoveries at RHIC", *Nucl. Phys. A* **757** (2005) 28, doi:10.1016/j.nuclphysa.2005.03.084, arXiv:nucl-ex/0410022.
- [3] STAR Collaboration, "Experimental and theoretical challenges in the search for the quark gluon plasma: The STAR Collaboration's critical assessment of the evidence from RHIC collisions", *Nucl. Phys. A* **757** (2005) 102, doi:10.1016/j.nuclphysa.2005.03.085, arXiv:nucl-ex/0501009.
- [4] PHENIX Collaboration, "Formation of dense partonic matter in relativistic nucleus-nucleus collisions at RHIC: Experimental evaluation by the PHENIX collaboration", *Nucl. Phys. A* **757** (2005) 184, doi:10.1016/j.nuclphysa.2005.03.086, arXiv:nucl-ex/0410003.
- [5] ALICE Collaboration, "Harmonic decomposition of two-particle angular correlations in Pb-Pb collisions at $\sqrt{s_{NN}} = 2.76$ TeV", *Phys. Lett. B* **708** (2012) 249, doi:10.1016/j.physletb.2012.01.060, arXiv:1109.2501.
- [6] ALICE Collaboration, "Elliptic flow of identified hadrons in Pb-Pb collisions at $\sqrt{s_{NN}} = 2.76$ TeV", (2014). arXiv:1405.4632.

- [7] ATLAS Collaboration, "Measurement of the azimuthal anisotropy for charged particle production in $\sqrt{s_{\text{NN}}} = 2.76$ TeV lead-lead collisions with the ATLAS detector", *Phys. Rev. C* **86** (2012) 014907, doi:10.1103/PhysRevC.86.014907, arXiv:1203.3087.
- [8] ATLAS Collaboration, "Measurement of the distributions of event-by-event flow harmonics in lead-lead collisions at $\sqrt{s_{\text{NN}}} = 2.76$ TeV with the ATLAS detector at the LHC", *JHEP* **11** (2013) 183, doi:10.1007/JHEP11(2013)183, arXiv:1305.2942.
- [9] ATLAS Collaboration, "Measurement of event-plane correlations in $\sqrt{s_{\text{NN}}} = 2.76$ TeV lead-lead collisions with the ATLAS detector", *Phys. Rev. C* **90** (2014) 024905, doi:10.1103/PhysRevC.90.024905, arXiv:1403.0489.
- [10] CMS Collaboration, "Centrality dependence of dihadron correlations and azimuthal anisotropy harmonics in PbPb collisions at $\sqrt{s_{\text{NN}}} = 2.76$ TeV", *Eur. Phys. J. C* **72** (2012) 2012, doi:10.1140/epjc/s10052-012-2012-3, arXiv:1201.3158.
- [11] CMS Collaboration, "Measurement of the elliptic anisotropy of charged particles produced in PbPb collisions at nucleon-nucleon center-of-mass energy = 2.76 TeV", *Phys. Rev. C* **87** (2013) 014902, doi:10.1103/PhysRevC.87.014902, arXiv:1204.1409.
- [12] CMS Collaboration, "Measurement of higher-order harmonic azimuthal anisotropy in PbPb collisions at $\sqrt{s_{\text{NN}}} = 2.76$ TeV", *Phys. Rev. C* **89** (2014) 044906, doi:10.1103/PhysRevC.89.044906, arXiv:1310.8651.
- [13] CMS Collaboration, "Studies of azimuthal dihadron correlations in ultra-central PbPb collisions at $\sqrt{s_{\text{NN}}} = 2.76$ TeV", *JHEP* **02** (2014) 088, doi:10.1007/JHEP02(2014)088, arXiv:1312.1845.
- [14] J.-Y. Ollitrault, "Determination of the reaction plane in ultrarelativistic nuclear collisions", *Phys. Rev. D* **48** (1993) 1132, doi:10.1103/PhysRevD.48.1132, arXiv:hep-ph/9303247.
- [15] S. Voloshin and Y. Zhang, "Flow study in relativistic nuclear collisions by Fourier expansion of azimuthal particle distributions", *Z. Phys. C* **70** (1996) 665, doi:10.1007/s002880050141, arXiv:hep-ph/9407282.
- [16] A. M. Poskanzer and S. A. Voloshin, "Methods for analyzing anisotropic flow in relativistic nuclear collisions", *Phys. Rev. C* **58** (1998) 1671, doi:10.1103/PhysRevC.58.1671, arXiv:nucl-ex/9805001.
- [17] B. Alver and G. Roland, "Collision geometry fluctuations and triangular flow in heavy-ion collisions", *Phys. Rev. C* **81** (2010) 054905, doi:10.1103/PhysRevC.81.054905, arXiv:1003.0194. [Erratum: doi:10.1103/PhysRevC.82.039903].
- [18] B. H. Alver, C. Gombeaud, M. Luzum, and J.-Y. Ollitrault, "Triangular flow in hydrodynamics and transport theory", *Phys. Rev. C* **82** (2010) 034913, doi:10.1103/PhysRevC.82.034913, arXiv:1007.5469.
- [19] B. Schenke, S. Jeon, and C. Gale, "Elliptic and triangular flow in event-by-event D=3+1 viscous hydrodynamics", *Phys. Rev. Lett.* **106** (2011) 042301, doi:10.1103/PhysRevLett.106.042301, arXiv:1009.3244.

- [20] Z. Qiu, C. Shen, and U. Heinz, “Hydrodynamic elliptic and triangular flow in Pb-Pb collisions at $\sqrt{s_{\text{NN}}} = 2.76$ TeV”, *Phys. Lett. B* **707** (2012) 151, doi:10.1016/j.physletb.2011.12.041, arXiv:1110.3033.
- [21] P. Danielewicz and G. Odyniec, “Transverse momentum analysis of collective motion in relativistic nuclear collisions”, *Phys. Lett. B* **157** (1985) 146, doi:10.1016/0370-2693(85)91535-7.
- [22] CMS Collaboration, “Multiplicity and transverse momentum dependence of two- and four-particle correlations in pPb and PbPb collisions”, *Phys. Lett. B* **724** (2013) 213, doi:10.1016/j.physletb.2013.06.028, arXiv:1305.0609.
- [23] F. G. Gardim, F. Grassi, M. Luzum, and J.-Y. Ollitrault, “Breaking of factorization of two-particle correlations in hydrodynamics”, *Phys. Rev. C* **87** (2013) 031901, doi:10.1103/PhysRevC.87.031901, arXiv:1211.0989.
- [24] U. Heinz, Z. Qiu, and C. Shen, “Fluctuating flow angles and anisotropic flow measurements”, *Phys. Rev. C* **87** (2013) 034913, doi:10.1103/PhysRevC.87.034913, arXiv:1302.3535.
- [25] I. Kozlov et al., “Transverse momentum structure of pair correlations as a signature of collective behavior in small collision systems”, (2014). arXiv:1405.3976.
- [26] S. Floerchinger and U. A. Wiedemann, “Mode-by-mode fluid dynamics for relativistic heavy ion collisions”, *Phys. Lett. B* **728** (2014) 407, doi:10.1016/j.physletb.2013.12.025, arXiv:1307.3453.
- [27] C. E. Coleman-Smith, H. Petersen, and R. L. Wolpert, “Classification of initial state granularity via 2d Fourier expansion”, *J. Phys. G* **40** (2013) 095103, doi:10.1088/0954-3899/40/9/095103, arXiv:1204.5774.
- [28] CMS Collaboration, “Observation of long-range near-side angular correlations in proton-proton collisions at the LHC”, *JHEP* **09** (2010) 091, doi:10.1007/JHEP09(2010)091, arXiv:1009.4122.
- [29] CMS Collaboration, “Observation of long-range near-side angular correlations in proton-lead collisions at the LHC”, *Phys. Lett. B* **718** (2013) 795, doi:10.1016/j.physletb.2012.11.025, arXiv:1210.5482.
- [30] ALICE Collaboration, “Long-range angular correlations on the near and away side in pPb collisions at $\sqrt{s_{\text{NN}}} = 5.02$ TeV”, *Phys. Lett. B* **719** (2013) 29, doi:10.1016/j.physletb.2013.01.012, arXiv:1212.2001.
- [31] ATLAS Collaboration, “Observation of Associated Near-Side and Away-Side Long-Range Correlations in $\sqrt{s_{\text{NN}}} = 5.02$ TeV Proton-Lead Collisions with the ATLAS Detector”, *Phys. Rev. Lett.* **110** (2013) 182302, doi:10.1103/PhysRevLett.110.182302, arXiv:1212.5198.
- [32] ATLAS Collaboration, “Measurement of long-range pseudorapidity correlations and azimuthal harmonics in $\sqrt{s_{\text{NN}}} = 5.02$ TeV proton-lead collisions with the ATLAS detector”, *Phys. Rev. C* **90** (2014) 044906, doi:10.1103/PhysRevC.90.044906, arXiv:1409.1792.

- [33] P. Bozek, W. Broniowski, and J. Moreira, “Torqued fireballs in relativistic heavy-ion collisions”, *Phys. Rev. C* **83** (2011) 034911, doi:10.1103/PhysRevC.83.034911, arXiv:1011.3354.
- [34] L.-G. Pang et al., “Longitudinal Decorrelation of Anisotropic Flows in Heavy-ion Collisions at the LHC”, (2014). arXiv:1410.8690.
- [35] K. Xiao, F. Liu, and F. Wang, “Event-plane decorrelation over pseudo-rapidity and its effect on azimuthal anisotropy measurement in relativistic heavy-ion collisions”, *Phys. Rev. C* **87** (2013) 011901, doi:10.1103/PhysRevC.87.011901, arXiv:1208.1195.
- [36] J. Jia and P. Huo, “A method for studying the rapidity fluctuation and decorrelation of harmonic flow in heavy-ion collisions”, *Phys. Rev. C* **90** (2014) 034905, doi:10.1103/PhysRevC.90.034905, arXiv:1402.6680.
- [37] CMS Collaboration, “The CMS experiment at the CERN LHC”, *JINST* **3** (2008) S08004, doi:10.1088/1748-0221/3/08/S08004.
- [38] GEANT4 Collaboration, “GEANT4—a simulation toolkit”, *Nucl. Instrum. Meth. A* **506** (2003) 250, doi:10.1016/S0168-9002(03)01368-8.
- [39] Ø. Djuvsland and J. Nystrand, “Single and double photonuclear excitations in Pb+Pb collisions at $\sqrt{s_{NN}} = 2.76$ TeV at the CERN Large Hadron Collider”, *Phys. Rev. C* **83** (2011) 041901, doi:10.1103/PhysRevC.83.041901, arXiv:1011.4908.
- [40] I. P. Lokhtin and A. M. Snigirev, “A model of jet quenching in ultrarelativistic heavy ion collisions and high- p_T hadron spectra at RHIC”, *Eur. Phys. J. C* **45** (2006) 211, doi:10.1140/epjc/s2005-02426-3, arXiv:hep-ph/0506189.
- [41] S. Porteboeuf, T. Pierog, and K. Werner, “Producing Hard Processes Regarding the Complete Event: The EPOS Event Generator”, (2010). arXiv:1006.2967.
- [42] M. Gyulassy and X.-N. Wang, “HIJING 1.0: A Monte Carlo program for parton and particle production in high-energy hadronic and nuclear collisions”, *Comput. Phys. Commun.* **83** (1994) 307, doi:10.1016/0010-4655(94)90057-4, arXiv:nucl-th/9502021.
- [43] CMS Collaboration, “Description and performance of track and primary-vertex reconstruction with the CMS tracker”, *JINST* **9** (2014) doi:10.1088/1748-0221/9/10/P10009, arXiv:1405.6569.
- [44] CMS Collaboration, “Long-range and short-range dihadron angular correlations in central PbPb collisions at a nucleon-nucleon center of mass energy of 2.76 TeV”, *JHEP* **07** (2011) 076, doi:10.1007/JHEP07(2011)076, arXiv:1105.2438.
- [45] CMS Collaboration, “Long-range two-particle correlations of strange hadrons with charged particles in pPb and PbPb collisions at LHC energies”, *Phys. Lett. B* **742** (2015) 200, doi:10.1016/j.physletb.2015.01.034, arXiv:1409.3392.
- [46] M. L. Miller, K. Reygers, S. J. Sanders, and P. Steinberg, “Glauber modeling in high energy nuclear collisions”, *Ann. Rev. Nucl. Part. Sci.* **57** (2007) 205, doi:10.1146/annurev.nucl.57.090506.123020, arXiv:nucl-ex/0701025.
- [47] B. Alver, M. Baker, C. Loizides, and P. Steinberg, “The PHOBOS Glauber Monte Carlo”, (2008). arXiv:0805.4411.

- [48] A. Adil et al., “The eccentricity in heavy-ion collisions from color glass condensate initial conditions”, *Phys. Rev. C* **74** (2006) 044905, doi:10.1103/PhysRevC.74.044905, arXiv:nucl-th/0605012.

A The CMS Collaboration

Yerevan Physics Institute, Yerevan, Armenia

V. Khachatryan, A.M. Sirunyan, A. Tumasyan

Institut für Hochenergiephysik der OeAW, Wien, Austria

W. Adam, E. Asilar, T. Bergauer, J. Brandstetter, M. Dragicevic, J. Erö, M. Flechl, M. Friedl, R. Frühwirth¹, V.M. Ghete, C. Hartl, N. Hörmann, J. Hrubec, M. Jeitler¹, W. Kiesenhofer, V. Knünz, A. König, M. Krammer¹, I. Krätschmer, D. Liko, I. Mikulec, D. Rabadý², B. Rahbaran, H. Rohringer, J. Schieck¹, R. Schöfbeck, J. Strauss, W. Treberer-Treberspurg, W. Waltenberger, C.-E. Wulz¹

National Centre for Particle and High Energy Physics, Minsk, Belarus

V. Mossolov, N. Shumeiko, J. Suarez Gonzalez

Universiteit Antwerpen, Antwerpen, Belgium

S. Alderweireldt, S. Bansal, T. Cornelis, E.A. De Wolf, X. Janssen, A. Knutsson, J. Lauwers, S. Luyckx, S. Ochesanu, R. Rougny, M. Van De Klundert, H. Van Haevermaet, P. Van Mechelen, N. Van Remortel, A. Van Spillbeeck

Vrije Universiteit Brussel, Brussel, Belgium

S. Abu Zeid, F. Blekman, J. D'Hondt, N. Daci, I. De Bruyn, K. Deroover, N. Heracleous, J. Keaveney, S. Lowette, L. Moreels, A. Olbrechts, Q. Python, D. Strom, S. Tavernier, W. Van Doninck, P. Van Mulders, G.P. Van Onsem, I. Van Parijs

Université Libre de Bruxelles, Bruxelles, Belgium

C. Caillol, B. Clerboux, G. De Lentdecker, H. Delannoy, D. Dobur, G. Fasanella, L. Favart, A.P.R. Gay, A. Grebenyuk, A. Léonard, A. Mohammadi, L. Perniè, A. Randle-conde, T. Reis, T. Seva, L. Thomas, C. Vander Velde, P. Vanlaer, J. Wang, F. Zenoni

Ghent University, Ghent, Belgium

K. Beernaert, L. Benucci, A. Cimmino, S. Crucy, A. Fagot, G. Garcia, M. Gul, J. Mccartin, A.A. Ocampo Rios, D. Poyraz, D. Ryckbosch, S. Salva Diblen, M. Sigamani, N. Strobbe, F. Thyssen, M. Tytgat, W. Van Driessche, E. Yazgan, N. Zaganidis

Université Catholique de Louvain, Louvain-la-Neuve, Belgium

S. Basegmez, C. Beluffi³, G. Bruno, R. Castello, A. Caudron, L. Ceard, G.G. Da Silveira, C. Delaere, T. du Pree, D. Favart, L. Forthomme, A. Giammanco⁴, J. Hollar, A. Jafari, P. Jez, M. Komm, V. Lemaitre, A. Mertens, C. Nuttens, L. Perrini, A. Pin, K. Piotrkowski, A. Popov⁵, L. Quertenmont, M. Selvaggi, M. Vidal Marono

Université de Mons, Mons, Belgium

N. Beliy, T. Caebergs, G.H. Hammad

Centro Brasileiro de Pesquisas Fisicas, Rio de Janeiro, Brazil

W.L. Aldá Júnior, G.A. Alves, L. Brito, M. Correa Martins Junior, T. Dos Reis Martins, C. Hensel, C. Mora Herrera, A. Moraes, M.E. Pol, P. Rebello Teles

Universidade do Estado do Rio de Janeiro, Rio de Janeiro, Brazil

E. Belchior Batista Das Chagas, W. Carvalho, J. Chinellato⁶, A. Custódio, E.M. Da Costa, D. De Jesus Damiao, C. De Oliveira Martins, S. Fonseca De Souza, L.M. Huertas Guativa, H. Malbouisson, D. Matos Figueiredo, L. Mundim, H. Nogima, W.L. Prado Da Silva, J. Santaolalla, A. Santoro, A. Sznajder, E.J. Tonelli Manganote⁶, A. Vilela Pereira

Universidade Estadual Paulista ^a, Universidade Federal do ABC ^b, São Paulo, Brazil

S. Ahuja, C.A. Bernardes^b, S. Dogra^a, T.R. Fernandez Perez Tomei^a, E.M. Gregores^b, P.G. Mercadante^b, S.F. Novaes^a, Sandra S. Padula^a, D. Romero Abad, J.C. Ruiz Vargas

Institute for Nuclear Research and Nuclear Energy, Sofia, Bulgaria

A. Aleksandrov, V. Genchev², R. Hadjiiska, P. Iaydjiev, A. Marinov, S. Piperov, M. Rodozov, S. Stoykova, G. Sultanov, M. Vutova

University of Sofia, Sofia, Bulgaria

A. Dimitrov, I. Glushkov, L. Litov, B. Pavlov, P. Petkov

Institute of High Energy Physics, Beijing, China

M. Ahmad, J.G. Bian, G.M. Chen, H.S. Chen, M. Chen, T. Cheng, R. Du, C.H. Jiang, R. Plestina⁷, F. Romeo, S.M. Shaheen, J. Tao, C. Wang, Z. Wang

State Key Laboratory of Nuclear Physics and Technology, Peking University, Beijing, China

C. Asawatrangkuldee, Y. Ban, G. Chen, Q. Li, S. Liu, Y. Mao, S.J. Qian, D. Wang, M. Wang, Q. Wang, Z. Xu, D. Yang, F. Zhang⁸, L. Zhang, Z. Zhang, W. Zou

Universidad de Los Andes, Bogota, Colombia

C. Avila, A. Cabrera, L.F. Chaparro Sierra, C. Florez, J.P. Gomez, B. Gomez Moreno, J.C. Sanabria

University of Split, Faculty of Electrical Engineering, Mechanical Engineering and Naval Architecture, Split, Croatia

N. Godinovic, D. Lelas, D. Polic, I. Puljak

University of Split, Faculty of Science, Split, Croatia

Z. Antunovic, M. Kovac

Institute Rudjer Boskovic, Zagreb, Croatia

V. Brigljevic, K. Kadija, J. Luetic, L. Sudic

University of Cyprus, Nicosia, Cyprus

A. Attikis, G. Mavromanolakis, J. Mousa, C. Nicolaou, F. Ptochos, P.A. Razis, H. Rykaczewski

Charles University, Prague, Czech Republic

M. Bodlak, M. Finger, M. Finger Jr.⁹

Academy of Scientific Research and Technology of the Arab Republic of Egypt, Egyptian Network of High Energy Physics, Cairo, Egypt

A. Ali¹⁰, R. Aly, S. Aly, Y. Assran¹¹, A. Ellithi Kamel¹², A. Lotfy, M.A. Mahmoud¹³, R. Masod¹⁰, A. Radi^{14,10}

National Institute of Chemical Physics and Biophysics, Tallinn, Estonia

B. Calpas, M. Kadastik, M. Murumaa, M. Raidal, A. Tiko, C. Veelken

Department of Physics, University of Helsinki, Helsinki, Finland

P. Eerola, M. Voutilainen

Helsinki Institute of Physics, Helsinki, Finland

J. Härkönen, V. Karimäki, R. Kinnunen, T. Lampén, K. Lassila-Perini, S. Lehti, T. Lindén, P. Luukka, T. Mäenpää, T. Peltola, E. Tuominen, J. Tuominiemi, E. Tuovinen, L. Wendland

Lappeenranta University of Technology, Lappeenranta, Finland

J. Talvitie, T. Tuuva

DSM/IRFU, CEA/Saclay, Gif-sur-Yvette, France

M. Besancon, F. Couderc, M. Dejardin, D. Denegri, B. Fabbro, J.L. Faure, C. Favaro, F. Ferri, S. Ganjour, A. Givernaud, P. Gras, G. Hamel de Monchenault, P. Jarry, E. Locci, J. Malcles, J. Rander, A. Rosowsky, M. Titov, A. Zghiche

Laboratoire Leprince-Ringuet, Ecole Polytechnique, IN2P3-CNRS, Palaiseau, France

S. Baffioni, F. Beaudette, P. Busson, L. Cadamuro, E. Chapon, C. Charlot, T. Dahms, O. Davignon, N. Filipovic, A. Florent, R. Granier de Cassagnac, L. Mastrolorenzo, P. Miné, I.N. Naranjo, M. Nguyen, C. Ochando, G. Ortona, P. Paganini, S. Regnard, R. Salerno, J.B. Sauvan, Y. Sirois, T. Strebler, Y. Yilmaz, A. Zabi

Institut Pluridisciplinaire Hubert Curien, Université de Strasbourg, Université de Haute Alsace Mulhouse, CNRS/IN2P3, Strasbourg, France

J.-L. Agram¹⁵, J. Andrea, A. Aubin, D. Bloch, J.-M. Brom, M. Buttignol, E.C. Chabert, N. Chanon, C. Collard, E. Conte¹⁵, J.-C. Fontaine¹⁵, D. Gelé, U. Goerlach, C. Goetzmann, A.-C. Le Bihan, J.A. Merlin², K. Skovpen, P. Van Hove

Centre de Calcul de l'Institut National de Physique Nucleaire et de Physique des Particules, CNRS/IN2P3, Villeurbanne, France

S. Gadrat

Université de Lyon, Université Claude Bernard Lyon 1, CNRS-IN2P3, Institut de Physique Nucléaire de Lyon, Villeurbanne, France

S. Beauceron, N. Beaupere, C. Bernet⁷, G. Boudoul², E. Bouvier, S. Brochet, C.A. Carrillo Montoya, J. Chasserat, R. Chierici, D. Contardo, B. Courbon, P. Depasse, H. El Mamouni, J. Fan, J. Fay, S. Gascon, M. Gouzevitch, B. Ille, I.B. Laktineh, M. Lethuillier, L. Mirabito, A.L. Pequegnot, S. Perries, J.D. Ruiz Alvarez, D. Sabes, L. Sgandurra, V. Sordini, M. Vander Donckt, P. Verdier, S. Viret, H. Xiao

Institute of High Energy Physics and Informatization, Tbilisi State University, Tbilisi, Georgia

I. Bagaturia¹⁶

RWTH Aachen University, I. Physikalisches Institut, Aachen, Germany

C. Autermann, S. Beranek, M. Bontenackels, M. Edelhoff, L. Feld, A. Heister, M.K. Kiesel, K. Klein, M. Lipinski, A. Ostapchuk, M. Preuten, F. Raupach, J. Sammet, S. Schael, J.F. Schulte, T. Verlage, H. Weber, B. Wittmer, V. Zhukov⁵

RWTH Aachen University, III. Physikalisches Institut A, Aachen, Germany

M. Ata, M. Brodski, E. Dietz-Laursonn, D. Duchardt, M. Endres, M. Erdmann, S. Erdweg, T. Esch, R. Fischer, A. Güth, T. Hebbeker, C. Heidemann, K. Hoepfner, D. Klingebiel, S. Knutzen, P. Kreuzer, M. Merschmeyer, A. Meyer, P. Millet, M. Olschewski, K. Padeken, P. Papacz, T. Pook, M. Radziej, H. Reithler, M. Rieger, S.A. Schmitz, L. Sonnenschein, D. Teyssier, S. Thüer

RWTH Aachen University, III. Physikalisches Institut B, Aachen, Germany

V. Cherepanov, Y. Erdogan, G. Flügge, H. Geenen, M. Geisler, W. Haj Ahmad, F. Hoehle, B. Kargoll, T. Kress, Y. Kuessel, A. Künsken, J. Lingemann², A. Nowack, I.M. Nugent, C. Pistone, O. Pooth, A. Stahl

Deutsches Elektronen-Synchrotron, Hamburg, Germany

M. Aldaya Martin, I. Asin, N. Bartosik, O. Behnke, U. Behrens, A.J. Bell, A. Bethani, K. Borras, A. Burgmeier, A. Cakir, L. Calligaris, A. Campbell, S. Choudhury, F. Costanza, C. Diez Pardos, G. Dolinska, S. Dooling, T. Dorland, G. Eckerlin, D. Eckstein, T. Eichhorn, G. Flucke, J. Garay

Garcia, A. Geiser, A. Gizhko, P. Gunnellini, J. Hauk, M. Hempel¹⁷, H. Jung, A. Kalogeropoulos, O. Karacheban¹⁷, M. Kasemann, P. Katsas, J. Kieseler, C. Kleinwort, I. Korol, W. Lange, J. Leonard, K. Lipka, A. Lobanov, R. Mankel, I. Marfin¹⁷, I.-A. Melzer-Pellmann, A.B. Meyer, G. Mittag, J. Mnich, A. Mussgiller, S. Naumann-Emme, A. Nayak, E. Ntomari, H. Perrey, D. Pitzl, R. Placakyte, A. Raspereza, P.M. Ribeiro Cipriano, B. Roland, E. Ron, M.Ö. Sahin, J. Salfeld-Nebgen, P. Saxena, T. Schoerner-Sadenius, M. Schröder, C. Seitz, S. Spannagel, C. Wissing

University of Hamburg, Hamburg, Germany

V. Blobel, M. Centis Vignali, A.R. Draeger, J. Erfle, E. Garutti, K. Goebel, D. Gonzalez, M. Görner, J. Haller, M. Hoffmann, R.S. Höing, A. Junkes, H. Kirschenmann, R. Klanner, R. Kogler, T. Lapsien, T. Lenz, I. Marchesini, D. Marconi, D. Nowatschin, J. Ott, T. Peiffer, A. Perieanu, N. Pietsch, J. Poehlsen, D. Rathjens, C. Sander, H. Schettler, P. Schleper, E. Schlieckau, A. Schmidt, M. Seidel, V. Sola, H. Stadie, G. Steinbrück, H. Tholen, D. Troendle, E. Usai, L. Vaneldereren, A. Vanhoefer

Institut für Experimentelle Kernphysik, Karlsruhe, Germany

M. Akbiyik, C. Barth, C. Baus, J. Berger, C. Böser, E. Butz, T. Chwalek, F. Colombo, W. De Boer, A. Descroix, A. Dierlamm, M. Feindt, F. Frensch, M. Giffels, A. Gilbert, F. Hartmann², U. Husemann, I. Katkov⁵, A. Kornmayer², P. Lobelle Pardo, M.U. Mozer, T. Müller, Th. Müller, M. Plagge, G. Quast, K. Rabbertz, S. Röcker, F. Roscher, H.J. Simonis, F.M. Stober, R. Ulrich, J. Wagner-Kuhr, S. Wayand, T. Weiler, C. Wöhrmann, R. Wolf

Institute of Nuclear and Particle Physics (INPP), NCSR Demokritos, Aghia Paraskevi, Greece

G. Anagnostou, G. Daskalakis, T. Gerasis, V.A. Giakoumopoulou, A. Kyriakis, D. Loukas, A. Markou, A. Psallidas, I. Topsis-Giotis

University of Athens, Athens, Greece

A. Agapitos, S. Kesisoglou, A. Panagiotou, N. Saoulidou, E. Tziaferi

University of Ioánnina, Ioánnina, Greece

I. Evangelou, G. Flouris, C. Foudas, P. Kokkas, N. Loukas, N. Manthos, I. Papadopoulos, E. Paradas, J. Strologas

Wigner Research Centre for Physics, Budapest, Hungary

G. Bencze, C. Hajdu, P. Hidas, D. Horvath¹⁸, F. Sikler, V. Veszpremi, G. Vesztergombi¹⁹, A.J. Zsigmond

Institute of Nuclear Research ATOMKI, Debrecen, Hungary

N. Beni, S. Czellar, J. Karancsi²⁰, J. Molnar, J. Palinkas, Z. Szillasi

University of Debrecen, Debrecen, Hungary

M. Bartók²¹, A. Makovec, P. Raics, Z.L. Trocsanyi

National Institute of Science Education and Research, Bhubaneswar, India

P. Mal, K. Mandal, N. Sahoo, S.K. Swain

Panjab University, Chandigarh, India

S.B. Beri, V. Bhatnagar, R. Chawla, R. Gupta, U. Bhawandeep, A.K. Kalsi, A. Kaur, M. Kaur, R. Kumar, A. Mehta, M. Mittal, N. Nishu, J.B. Singh

University of Delhi, Delhi, India

Ashok Kumar, Arun Kumar, A. Bhardwaj, B.C. Choudhary, A. Kumar, S. Malhotra, M. Naimuddin, K. Ranjan, R. Sharma, V. Sharma

Saha Institute of Nuclear Physics, Kolkata, India

S. Banerjee, S. Bhattacharya, K. Chatterjee, S. Dutta, B. Gomber, Sa. Jain, Sh. Jain, R. Khurana, N. Majumdar, A. Modak, K. Mondal, S. Mukherjee, S. Mukhopadhyay, A. Roy, D. Roy, S. Roy Chowdhury, S. Sarkar, M. Sharan

Bhabha Atomic Research Centre, Mumbai, India

A. Abdulsalam, D. Dutta, V. Jha, V. Kumar, A.K. Mohanty², L.M. Pant, P. Shukla, A. Topkar

Tata Institute of Fundamental Research, Mumbai, India

T. Aziz, S. Banerjee, S. Bhowmik²², R.M. Chatterjee, R.K. Dewanjee, S. Dugad, S. Ganguly, S. Ghosh, M. Guchait, A. Gurtu²³, G. Kole, S. Kumar, M. Maity²², G. Majumder, K. Mazumdar, G.B. Mohanty, B. Parida, K. Sudhakar, N. Sur, B. Sutar, N. Wickramage²⁴

Indian Institute of Science Education and Research (IISER), Pune, India

S. Sharma

Institute for Research in Fundamental Sciences (IPM), Tehran, Iran

H. Bakhshiansohi, H. Behnamian, S.M. Etesami²⁵, A. Fahim²⁶, R. Goldouzian, M. Khakzad, M. Mohammadi Najafabadi, M. Naseri, S. Paktinat Mehdiabadi, F. Rezaei Hosseinabadi, B. Safarzadeh²⁷, M. Zeinali

University College Dublin, Dublin, Ireland

M. Felcini, M. Grunewald

INFN Sezione di Bari ^a, Università di Bari ^b, Politecnico di Bari ^c, Bari, Italy

M. Abbrescia^{a,b}, C. Calabria^{a,b}, C. Caputo^{a,b}, S.S. Chhibra^{a,b}, A. Colaleo^a, D. Creanza^{a,c}, L. Cristella^{a,b}, N. De Filippis^{a,c}, M. De Palma^{a,b}, L. Fiore^a, G. Iaselli^{a,c}, G. Maggi^{a,c}, M. Maggi^a, G. Miniello^{a,b}, S. My^{a,c}, S. Nuzzo^{a,b}, A. Pompili^{a,b}, G. Pugliese^{a,c}, R. Radogna^{a,b,2}, A. Ranieri^a, G. Selvaggi^{a,b}, A. Sharma^a, L. Silvestris^{a,2}, R. Venditti^{a,b}, P. Verwilligen^a

INFN Sezione di Bologna ^a, Università di Bologna ^b, Bologna, Italy

G. Abbiendi^a, C. Battilana, A.C. Benvenuti^a, D. Bonacorsi^{a,b}, S. Braibant-Giacomelli^{a,b}, L. Brigliadori^{a,b}, R. Campanini^{a,b}, P. Capiluppi^{a,b}, A. Castro^{a,b}, F.R. Cavallo^a, G. Codispoti^{a,b}, M. Cuffiani^{a,b}, G.M. Dallavalle^a, F. Fabbri^a, A. Fanfani^{a,b}, D. Fasanella^{a,b}, P. Giacomelli^a, C. Grandi^a, L. Guiducci^{a,b}, S. Marcellini^a, G. Masetti^a, A. Montanari^a, F.L. Navarria^{a,b}, A. Perrotta^a, A.M. Rossi^{a,b}, T. Rovelli^{a,b}, G.P. Siroli^{a,b}, N. Tosi^{a,b}, R. Travaglini^{a,b}

INFN Sezione di Catania ^a, Università di Catania ^b, CSFNSM ^c, Catania, Italy

G. Cappello^a, M. Chiorboli^{a,b}, S. Costa^{a,b}, F. Giordano^{a,2}, R. Potenza^{a,b}, A. Tricomi^{a,b}, C. Tuve^{a,b}

INFN Sezione di Firenze ^a, Università di Firenze ^b, Firenze, Italy

G. Barbagli^a, V. Ciulli^{a,b}, C. Civinini^a, R. D'Alessandro^{a,b}, E. Focardi^{a,b}, E. Gallo^a, S. Gonzi^{a,b}, V. Gori^{a,b}, P. Lenzi^{a,b}, M. Meschini^a, S. Paoletti^a, G. Sguazzoni^a, A. Tropiano^{a,b}

INFN Laboratori Nazionali di Frascati, Frascati, Italy

L. Benussi, S. Bianco, F. Fabbri, D. Piccolo

INFN Sezione di Genova ^a, Università di Genova ^b, Genova, Italy

V. Calvelli^{a,b}, F. Ferro^a, M. Lo Vetere^{a,b}, E. Robutti^a, S. Tosi^{a,b}

INFN Sezione di Milano-Bicocca ^a, Università di Milano-Bicocca ^b, Milano, Italy

M.E. Dinardo^{a,b}, S. Fiorendi^{a,b}, S. Gennai^{a,2}, R. Gerosa^{a,b}, A. Ghezzi^{a,b}, P. Govoni^{a,b}, M.T. Lucchini^{a,b,2}, S. Malvezzi^a, R.A. Manzoni^{a,b}, B. Marzocchi^{a,b,2}, D. Menasce^a, L. Moroni^a, M. Paganoni^{a,b}, D. Pedrini^a, S. Ragazzi^{a,b}, N. Redaelli^a, T. Tabarelli de Fatis^{a,b}

INFN Sezione di Napoli ^a, Università di Napoli 'Federico II' ^b, Napoli, Italy, Università della Basilicata ^c, Potenza, Italy, Università G. Marconi ^d, Roma, Italy

S. Buontempo^a, N. Cavallo^{a,c}, S. Di Guida^{a,d,2}, M. Esposito^{a,b}, F. Fabozzi^{a,c}, A.O.M. Iorio^{a,b}, G. Lanza^a, L. Lista^a, S. Meola^{a,d,2}, M. Merola^a, P. Paolucci^{a,2}, C. Sciacca^{a,b}

INFN Sezione di Padova ^a, Università di Padova ^b, Padova, Italy, Università di Trento ^c, Trento, Italy

P. Azzi^{a,2}, N. Bacchetta^a, D. Bisello^{a,b}, A. Branca^{a,b}, R. Carlin^{a,b}, A. Carvalho Antunes De Oliveira^{a,b}, P. Checchia^a, M. Dall'Osso^{a,b}, T. Dorigo^a, U. Gasparini^{a,b}, A. Gozzelino^a, K. Kanishchev^{a,c}, S. Lacaprara^a, M. Margoni^{a,b}, A.T. Meneguzzo^{a,b}, J. Pazzini^{a,b}, M. Pegoraro^a, N. Pozzobon^{a,b}, P. Ronchese^{a,b}, F. Simonetto^{a,b}, E. Torassa^a, M. Tosi^{a,b}, S. Vanini^{a,b}, S. Ventura^a, M. Zanetti, P. Zotto^{a,b}, A. Zucchetta^{a,b}

INFN Sezione di Pavia ^a, Università di Pavia ^b, Pavia, Italy

M. Gabusi^{a,b}, A. Magnani^a, S.P. Ratti^{a,b}, V. Re^a, C. Riccardi^{a,b}, P. Salvini^a, I. Vai^a, P. Vitulo^{a,b}

INFN Sezione di Perugia ^a, Università di Perugia ^b, Perugia, Italy

L. Alunni Solestizi^{a,b}, M. Biasini^{a,b}, G.M. Bilei^a, D. Ciangottini^{a,b,2}, L. Fanò^{a,b}, P. Lariccia^{a,b}, G. Mantovani^{a,b}, M. Menichelli^a, A. Saha^a, A. Santocchia^{a,b}, A. Spiezia^{a,b,2}

INFN Sezione di Pisa ^a, Università di Pisa ^b, Scuola Normale Superiore di Pisa ^c, Pisa, Italy

K. Androsov^{a,28}, P. Azzurri^a, G. Bagliesi^a, J. Bernardini^a, T. Boccali^a, G. Broccoli^{a,c}, R. Castaldi^a, M.A. Ciocci^{a,28}, R. Dell'Orso^a, S. Donato^{a,c,2}, G. Fedi, F. Fiori^{a,c}, L. Foà^{a,c†}, A. Giassi^a, M.T. Grippo^{a,28}, F. Ligabue^{a,c}, T. Lomtadze^a, L. Martini^{a,b}, A. Messineo^{a,b}, C.S. Moon^{a,29}, F. Palla^a, A. Rizzi^{a,b}, A. Savoy-Navarro^{a,30}, A.T. Serban^a, P. Spagnolo^a, P. Squillacioti^{a,28}, R. Tenchini^a, G. Tonelli^{a,b}, A. Venturi^a, P.G. Verdini^a

INFN Sezione di Roma ^a, Università di Roma ^b, Roma, Italy

L. Barone^{a,b}, F. Cavallari^a, G. D'imperio^{a,b}, D. Del Re^{a,b}, M. Diemoz^a, S. Gelli^{a,b}, C. Jorda^a, E. Longo^{a,b}, F. Margaroli^{a,b}, P. Meridiani^a, F. Micheli^{a,b}, G. Organtini^{a,b}, R. Paramatti^a, F. Preiato^{a,b}, S. Rahatlou^{a,b}, C. Rovelli^a, F. Santanastasio^{a,b}, L. Soffi^{a,b}, P. Traczyk^{a,b,2}

INFN Sezione di Torino ^a, Università di Torino ^b, Torino, Italy, Università del Piemonte Orientale ^c, Novara, Italy

N. Amapane^{a,b}, R. Arcidiacono^{a,c}, S. Argiro^{a,b}, M. Arneodo^{a,c}, R. Bellan^{a,b}, C. Biino^a, N. Cartiglia^a, S. Casasso^{a,b}, M. Costa^{a,b}, R. Covarelli, A. Degano^{a,b}, N. Demaria^a, L. Finco^{a,b,2}, B. Kiani^{a,b}, C. Mariotti^a, S. Maselli^a, E. Migliore^{a,b}, V. Monaco^{a,b}, M. Musich^a, M.M. Obertino^{a,c}, L. Pacher^{a,b}, N. Pastrone^a, M. Pelliccioni^a, G.L. Pinna Angioni^{a,b}, A. Romero^{a,b}, M. Ruspa^{a,c}, R. Sacchi^{a,b}, A. Solano^{a,b}, A. Staiano^a, U. Tamponi^a

INFN Sezione di Trieste ^a, Università di Trieste ^b, Trieste, Italy

S. Belforte^a, V. Candelise^{a,b,2}, M. Casarsa^a, F. Cossutti^a, G. Della Ricca^{a,b}, B. Gobbo^a, C. La Licata^{a,b}, M. Marone^{a,b}, A. Schizzi^{a,b}, T. Umer^{a,b}, A. Zanetti^a

Kangwon National University, Chunchon, Korea

S. Chang, A. Kropivnitskaya, S.K. Nam

Kyungpook National University, Daegu, Korea

D.H. Kim, G.N. Kim, M.S. Kim, D.J. Kong, S. Lee, Y.D. Oh, H. Park, A. Sakharov, D.C. Son

Chonbuk National University, Jeonju, Korea

H. Kim, T.J. Kim, M.S. Ryu

Chonnam National University, Institute for Universe and Elementary Particles, Kwangju, Korea

S. Song

Korea University, Seoul, Korea

S. Choi, Y. Go, D. Gyun, B. Hong, M. Jo, H. Kim, Y. Kim, B. Lee, K. Lee, K.S. Lee, S. Lee, S.K. Park, Y. Roh

Seoul National University, Seoul, Korea

H.D. Yoo

University of Seoul, Seoul, Korea

M. Choi, J.H. Kim, J.S.H. Lee, I.C. Park, G. Ryu

Sungkyunkwan University, Suwon, Korea

Y. Choi, Y.K. Choi, J. Goh, D. Kim, E. Kwon, J. Lee, I. Yu

Vilnius University, Vilnius, Lithuania

A. Juodagalvis, J. Vaitkus

National Centre for Particle Physics, Universiti Malaya, Kuala Lumpur, Malaysia

Z.A. Ibrahim, J.R. Komaragiri, M.A.B. Md Ali³¹, F. Mohamad Idris, W.A.T. Wan Abdullah

Centro de Investigacion y de Estudios Avanzados del IPN, Mexico City, Mexico

E. Casimiro Linares, H. Castilla-Valdez, E. De La Cruz-Burelo, I. Heredia-de La Cruz, A. Hernandez-Almada, R. Lopez-Fernandez, G. Ramirez Sanchez, A. Sanchez-Hernandez

Universidad Iberoamericana, Mexico City, Mexico

S. Carrillo Moreno, F. Vazquez Valencia

Benemerita Universidad Autonoma de Puebla, Puebla, Mexico

S. Carpinteyro, I. Pedraza, H.A. Salazar Ibarguen

Universidad Autónoma de San Luis Potosí, San Luis Potosí, Mexico

A. Morelos Pineda

University of Auckland, Auckland, New Zealand

D. Krofcheck

University of Canterbury, Christchurch, New Zealand

P.H. Butler, S. Reucroft

National Centre for Physics, Quaid-I-Azam University, Islamabad, Pakistan

A. Ahmad, M. Ahmad, Q. Hassan, H.R. Hoorani, W.A. Khan, T. Khurshid, M. Shoaib

National Centre for Nuclear Research, Swierk, Poland

H. Bialkowska, M. Bluj, B. Boimska, T. Frueboes, M. Górski, M. Kazana, K. Nawrocki, K. Romanowska-Rybinska, M. Szleper, P. Zalewski

Institute of Experimental Physics, Faculty of Physics, University of Warsaw, Warsaw, Poland

G. Brona, K. Bunkowski, K. Doroba, A. Kalinowski, M. Konecki, J. Krolikowski, M. Misiura, M. Olszewski, M. Walczak

Laboratório de Instrumentação e Física Experimental de Partículas, Lisboa, Portugal

P. Bargassa, C. Beirão Da Cruz E Silva, A. Di Francesco, P. Faccioli, P.G. Ferreira Parracho, M. Gallinaro, L. Lloret Iglesias, F. Nguyen, J. Rodrigues Antunes, J. Seixas, O. Toldaiev, D. Vadrucio, J. Varela, P. Vischia

Joint Institute for Nuclear Research, Dubna, Russia

S. Afanasiev, P. Bunin, M. Gavrilenko, I. Golutvin, I. Gorbunov, A. Kamenev, V. Karjavin, V. Konoplyanikov, A. Lanev, A. Malakhov, V. Matveev³², P. Moisezenz, V. Palichik, V. Perelygin, S. Shmatov, S. Shulha, N. Skatchkov, V. Smirnov, T. Toriashvili³³, A. Zarubin

Petersburg Nuclear Physics Institute, Gatchina (St. Petersburg), Russia

V. Golovtsov, Y. Ivanov, V. Kim³⁴, E. Kuznetsova, P. Levchenko, V. Murzin, V. Oreshkin, I. Smirnov, V. Sulimov, L. Uvarov, S. Vavilov, A. Vorobyev

Institute for Nuclear Research, Moscow, Russia

Yu. Andreev, A. Dermenev, S. Gninenko, N. Golubev, A. Karneyeu, M. Kirsanov, N. Krasnikov, A. Pashenkov, D. Tlisov, A. Toropin

Institute for Theoretical and Experimental Physics, Moscow, Russia

V. Epshteyn, V. Gavrillov, N. Lychkovskaya, V. Popov, I. Pozdnyakov, G. Safronov, A. Spiridonov, E. Vlasov, A. Zhokin

P.N. Lebedev Physical Institute, Moscow, Russia

V. Andreev, M. Azarkin³⁵, I. Dremin³⁵, M. Kirakosyan, A. Leonidov³⁵, G. Mesyats, S.V. Rusakov, A. Vinogradov

Skobeltsyn Institute of Nuclear Physics, Lomonosov Moscow State University, Moscow, Russia

A. Baskakov, A. Belyaev, E. Boos, A. Demiyanov, A. Ershov, A. Gribushin, O. Kodolova, V. Korotkikh, I. Lokhtin, I. Myagkov, S. Obraztsov, S. Petrushanko, V. Savrin, A. Snigirev, I. Vardanyan

State Research Center of Russian Federation, Institute for High Energy Physics, Protvino, Russia

I. Azhgirey, I. Bayshev, S. Bitioukov, V. Kachanov, A. Kalinin, D. Konstantinov, V. Krychkin, V. Petrov, R. Ryutin, A. Sobol, L. Tourtchanovitch, S. Troshin, N. Tyurin, A. Uzunian, A. Volkov

University of Belgrade, Faculty of Physics and Vinca Institute of Nuclear Sciences, Belgrade, Serbia

P. Adzic³⁶, D. Devetak, M. Ekmedzic, J. Milosevic, V. Rekovic

Centro de Investigaciones Energéticas Medioambientales y Tecnológicas (CIEMAT), Madrid, Spain

J. Alcaraz Maestre, E. Calvo, M. Cerrada, M. Chamizo Llatas, N. Colino, B. De La Cruz, A. Delgado Peris, D. Domínguez Vázquez, A. Escalante Del Valle, C. Fernandez Bedoya, J.P. Fernández Ramos, J. Flix, M.C. Fouz, P. Garcia-Abia, O. Gonzalez Lopez, S. Goy Lopez, J.M. Hernandez, M.I. Josa, E. Navarro De Martino, A. Pérez-Calero Yzquierdo, J. Puerta Pelayo, A. Quintario Olmeda, I. Redondo, L. Romero, M.S. Soares

Universidad Autónoma de Madrid, Madrid, Spain

C. Albajar, J.F. de Trocóniz, M. Missiroli, D. Moran

Universidad de Oviedo, Oviedo, Spain

H. Brun, J. Cuevas, J. Fernandez Menendez, S. Folgueras, I. Gonzalez Caballero, E. Palencia Cortezon, J.M. Vizan Garcia

Instituto de Física de Cantabria (IFCA), CSIC-Universidad de Cantabria, Santander, Spain

J.A. Brochero Cifuentes, I.J. Cabrillo, A. Calderon, J.R. Castiñeiras De Saa, J. Duarte Campderros, M. Fernandez, G. Gomez, A. Graziano, A. Lopez Virto, J. Marco, R. Marco,

C. Martinez Rivero, F. Matorras, F.J. Munoz Sanchez, J. Piedra Gomez, T. Rodrigo, A.Y. Rodríguez-Marrero, A. Ruiz-Jimeno, L. Scodellaro, I. Vila, R. Vilar Cortabitarte

CERN, European Organization for Nuclear Research, Geneva, Switzerland

D. Abbaneo, E. Auffray, G. Auzinger, M. Bachtis, P. Baillon, A.H. Ball, D. Barney, A. Benaglia, J. Bendavid, L. Benhabib, J.F. Benitez, G.M. Berruti, P. Bloch, A. Bocci, A. Bonato, C. Botta, H. Breuker, T. Camporesi, G. Cerminara, S. Colafranceschi³⁷, M. D'Alfonso, D. d'Enterria, A. Dabrowski, V. Daponte, A. David, M. De Gruttola, F. De Guio, A. De Roeck, S. De Visscher, E. Di Marco, M. Dobson, M. Dordevic, N. Dupont-Sagorin, A. Elliott-Peisert, G. Franzoni, W. Funk, D. Gigi, K. Gill, D. Giordano, M. Girone, F. Glege, R. Guida, S. Gundacker, M. Guthoff, J. Hammer, M. Hansen, P. Harris, J. Hegeman, V. Innocente, P. Janot, M.J. Kortelainen, K. Kousouris, K. Krajczar, P. Lecoq, C. Lourenço, N. Magini, L. Malgeri, M. Mannelli, J. Marrouche, A. Martelli, L. Masetti, F. Meijers, S. Mersi, E. Meschi, F. Moortgat, S. Morovic, M. Mulders, M.V. Nemallapudi, H. Neugebauer, S. Orfanelli, L. Orsini, L. Pape, E. Perez, A. Petrilli, G. Petrucciani, A. Pfeiffer, D. Piparo, A. Racz, G. Rolandi³⁸, M. Rovere, M. Ruan, H. Sakulin, C. Schäfer, C. Schwick, A. Sharma, P. Silva, M. Simon, P. Sphicas³⁹, D. Spiga, J. Steggemann, B. Stieger, M. Stoye, Y. Takahashi, D. Treille, A. Tsirou, G.I. Veres¹⁹, N. Wardle, H.K. Wöhri, A. Zagodzinska⁴⁰, W.D. Zeuner

Paul Scherrer Institut, Villigen, Switzerland

W. Bertl, K. Deiters, W. Erdmann, R. Horisberger, Q. Ingram, H.C. Kaestli, D. Kotlinski, U. Langenegger, T. Rohe

Institute for Particle Physics, ETH Zurich, Zurich, Switzerland

F. Bachmair, L. Bäni, L. Bianchini, M.A. Buchmann, B. Casal, G. Dissertori, M. Dittmar, M. Donegà, M. Dünser, P. Eller, C. Grab, C. Heidegger, D. Hits, J. Hoss, G. Kasieczka, W. Lustermann, B. Mangano, A.C. Marini, M. Marionneau, P. Martinez Ruiz del Arbol, M. Masciovecchio, D. Meister, N. Mohr, P. Musella, F. Nessi-Tedaldi, F. Pandolfi, J. Pata, F. Pauss, L. Perrozzi, M. Peruzzi, M. Quittnat, M. Rossini, A. Starodumov⁴¹, M. Takahashi, V.R. Tavolaro, K. Theofilatos, R. Wallny, H.A. Weber

Universität Zürich, Zurich, Switzerland

T.K. Aarrestad, C. AMSler⁴², M.F. Canelli, V. Chiochia, A. De Cosa, C. Galloni, A. Hinzmann, T. Hreus, B. Kilminster, C. Lange, J. Ngadiuba, D. Pinna, P. Robmann, F.J. Ronga, D. Salerno, S. Taroni, Y. Yang

National Central University, Chung-Li, Taiwan

M. Cardaci, K.H. Chen, T.H. Doan, C. Ferro, M. Konyushikhin, C.M. Kuo, W. Lin, Y.J. Lu, R. Volpe, S.S. Yu

National Taiwan University (NTU), Taipei, Taiwan

P. Chang, Y.H. Chang, Y. Chao, K.F. Chen, P.H. Chen, C. Dietz, U. Grundler, W.-S. Hou, Y. Hsiung, Y.F. Liu, R.-S. Lu, M. Miñano Moya, E. Petrakou, J.f. Tsai, Y.M. Tzeng, R. Wilken

Chulalongkorn University, Faculty of Science, Department of Physics, Bangkok, Thailand

B. Asavapibhop, G. Singh, N. Srimanobhas, N. Suwonjandee

Cukurova University, Adana, Turkey

A. Adiguzel, S. Cerci⁴³, C. Dozen, S. Girgis, G. Gokbulut, Y. Guler, E. Gurpinar, I. Hos, E.E. Kangal⁴⁴, A. Kayis Topaksu, G. Onengut⁴⁵, K. Ozdemir⁴⁶, S. Ozturk⁴⁷, B. Tali⁴³, H. Topakli⁴⁷, M. Vergili, C. Zorbilmez

Middle East Technical University, Physics Department, Ankara, Turkey

I.V. Akin, B. Bilin, S. Bilmis, B. Isildak⁴⁸, G. Karapinar⁴⁹, U.E. Surat, M. Yalvac, M. Zeyrek

Bogazici University, Istanbul, Turkey

E.A. Albayrak⁵⁰, E. Gülmez, M. Kaya⁵¹, O. Kaya⁵², T. Yetkin⁵³

Istanbul Technical University, Istanbul, Turkey

K. Cankocak, Y.O. Günaydin⁵⁴, F.I. Vardarli

Institute for Scintillation Materials of National Academy of Science of Ukraine, Kharkov, Ukraine

B. Grynyov

National Scientific Center, Kharkov Institute of Physics and Technology, Kharkov, Ukraine

L. Levchuk, P. Sorokin

University of Bristol, Bristol, United Kingdom

R. Aggleton, F. Ball, L. Beck, J.J. Brooke, E. Clement, D. Cussans, H. Flacher, J. Goldstein, M. Grimes, G.P. Heath, H.F. Heath, J. Jacob, L. Kreczko, C. Lucas, Z. Meng, D.M. Newbold⁵⁵, S. Paramesvaran, A. Poll, T. Sakuma, S. Seif El Nasr-storey, S. Senkin, D. Smith, V.J. Smith

Rutherford Appleton Laboratory, Didcot, United Kingdom

A. Belyaev⁵⁶, C. Brew, R.M. Brown, D.J.A. Cockerill, J.A. Coughlan, K. Harder, S. Harper, E. Olaiya, D. Petyt, C.H. Shepherd-Themistocleous, A. Thea, I.R. Tomalin, T. Williams, W.J. Womersley, S.D. Worm

Imperial College, London, United Kingdom

M. Baber, R. Bainbridge, O. Buchmuller, A. Bundock, D. Burton, M. Citron, D. Colling, L. Corpe, N. Cripps, P. Dauncey, G. Davies, A. De Wit, M. Della Negra, P. Dunne, A. Elwood, W. Ferguson, J. Fulcher, D. Futyan, G. Hall, G. Iles, M. Jarvis, G. Karapostoli, M. Kenzie, R. Lane, R. Lucas⁵⁵, L. Lyons, A.-M. Magnan, S. Malik, B. Mathias, J. Nash, A. Nikitenko⁴¹, J. Pela, M. Pesaresi, K. Petridis, D.M. Raymond, A. Richards, S. Rogerson, A. Rose, C. Seez, P. Sharp[†], A. Tapper, K. Uchida, M. Vazquez Acosta, T. Virdee, S.C. Zenz

Brunel University, Uxbridge, United Kingdom

J.E. Cole, P.R. Hobson, A. Khan, P. Kyberd, D. Leggat, D. Leslie, I.D. Reid, P. Symonds, L. Teodorescu, M. Turner

Baylor University, Waco, USA

J. Dittmann, K. Hatakeyama, A. Kasmi, H. Liu, N. Pastika, T. Scarborough, Z. Wu

The University of Alabama, Tuscaloosa, USA

O. Charaf, S.I. Cooper, C. Henderson, P. Rumerio

Boston University, Boston, USA

A. Avetisyan, T. Bose, C. Fantasia, D. Gastler, P. Lawson, D. Rankin, C. Richardson, J. Rohlf, J. St. John, L. Sulak, D. Zou

Brown University, Providence, USA

J. Alimena, E. Berry, S. Bhattacharya, D. Cutts, Z. Demiragli, N. Dhingra, A. Ferapontov, A. Garabedian, U. Heintz, E. Laird, G. Landsberg, Z. Mao, M. Narain, S. Sagir, T. Sinthuprasith

University of California, Davis, Davis, USA

R. Breedon, G. Breto, M. Calderon De La Barca Sanchez, S. Chauhan, M. Chertok, J. Conway, R. Conway, P.T. Cox, R. Erbacher, M. Gardner, W. Ko, R. Lander, M. Mulhearn, D. Pellett, J. Pilot, F. Ricci-Tam, S. Shalhout, J. Smith, M. Squires, D. Stolp, M. Tripathi, S. Wilbur, R. Yohay

University of California, Los Angeles, USA

R. Cousins, P. Everaerts, C. Farrell, J. Hauser, M. Ignatenko, G. Rakness, D. Saltzberg, E. Takasugi, V. Valuev, M. Weber

University of California, Riverside, Riverside, USA

K. Burt, R. Clare, J. Ellison, J.W. Gary, G. Hanson, J. Heilman, M. Ivova Rikova, P. Jandir, E. Kennedy, F. Lacroix, O.R. Long, A. Luthra, M. Malberti, M. Olmedo Negrete, A. Shrinivas, S. Sumowidagdo, H. Wei, S. Wimpenny

University of California, San Diego, La Jolla, USA

J.G. Branson, G.B. Cerati, S. Cittolin, R.T. D'Agnolo, A. Holzner, R. Kelley, D. Klein, D. Kovalskyi, J. Letts, I. Macneill, D. Olivito, S. Padhi, C. Palmer, M. Pieri, M. Sani, V. Sharma, S. Simon, M. Tadel, Y. Tu, A. Vartak, S. Wasserbaech⁵⁷, C. Welke, F. Würthwein, A. Yagil, G. Zevi Della Porta

University of California, Santa Barbara, Santa Barbara, USA

D. Barge, J. Bradmiller-Feld, C. Campagnari, A. Dishaw, V. Dutta, K. Flowers, M. Franco Sevilla, P. Geffert, C. George, F. Golf, L. Gouskos, J. Gran, J. Incandela, C. Justus, N. Mccoll, S.D. Mullin, J. Richman, D. Stuart, W. To, C. West, J. Yoo

California Institute of Technology, Pasadena, USA

D. Anderson, A. Apresyan, A. Bornheim, J. Bunn, Y. Chen, J. Duarte, A. Mott, H.B. Newman, C. Pena, M. Pierini, M. Spiropulu, J.R. Vlimant, S. Xie, R.Y. Zhu

Carnegie Mellon University, Pittsburgh, USA

V. Azzolini, A. Calamba, B. Carlson, T. Ferguson, Y. Iiyama, M. Paulini, J. Russ, M. Sun, H. Vogel, I. Vorobiev

University of Colorado at Boulder, Boulder, USA

J.P. Cumalat, W.T. Ford, A. Gaz, F. Jensen, A. Johnson, M. Krohn, T. Mulholland, U. Nauenberg, J.G. Smith, K. Stenson, S.R. Wagner

Cornell University, Ithaca, USA

J. Alexander, A. Chatterjee, J. Chaves, J. Chu, S. Dittmer, N. Eggert, N. Mirman, G. Nicolas Kaufman, J.R. Patterson, A. Ryd, L. Skinnari, W. Sun, S.M. Tan, W.D. Teo, J. Thom, J. Thompson, J. Tucker, Y. Weng, P. Wittich

Fermi National Accelerator Laboratory, Batavia, USA

S. Abdullin, M. Albrow, J. Anderson, G. Apollinari, L.A.T. Bauerdick, A. Beretvas, J. Berryhill, P.C. Bhat, G. Bolla, K. Burkett, J.N. Butler, H.W.K. Cheung, F. Chlebana, S. Cihangir, V.D. Elvira, I. Fisk, J. Freeman, E. Gottschalk, L. Gray, D. Green, S. Grünendahl, O. Gutsche, J. Hanlon, D. Hare, R.M. Harris, J. Hirschauer, B. Hooberman, Z. Hu, S. Jindariani, M. Johnson, U. Joshi, A.W. Jung, B. Klima, B. Kreis, S. Kwan[†], S. Lammel, J. Linacre, D. Lincoln, R. Lipton, T. Liu, R. Lopes De Sá, J. Lykken, K. Maeshima, J.M. Marraffino, V.I. Martinez Outschoorn, S. Maruyama, D. Mason, P. McBride, P. Merkel, K. Mishra, S. Mrenna, S. Nahn, C. Newman-Holmes, V. O'Dell, O. Prokofyev, E. Sexton-Kennedy, A. Soha, W.J. Spalding, L. Spiegel, L. Taylor, S. Tkaczyk, N.V. Tran, L. Uplegger, E.W. Vaandering, C. Vernieri, M. Verzocchi, R. Vidal, A. Whitbeck, F. Yang, H. Yin

University of Florida, Gainesville, USA

D. Acosta, P. Avery, P. Bortignon, D. Bourilkov, A. Carnes, M. Carver, D. Curry, S. Das, G.P. Di Giovanni, R.D. Field, M. Fisher, I.K. Furic, J. Hugon, J. Konigsberg, A. Korytov, T. Kypreos, J.F. Low, P. Ma, K. Matchev, H. Mei, P. Milenovic⁵⁸, G. Mitselmakher, L. Muniz, D. Rank, A. Rinkevicius, L. Shchutska, M. Snowball, D. Sperka, S.J. Wang, J. Yelton

Florida International University, Miami, USA

S. Hewamanage, S. Linn, P. Markowitz, G. Martinez, J.L. Rodriguez

Florida State University, Tallahassee, USA

A. Ackert, J.R. Adams, T. Adams, A. Askew, J. Bochenek, B. Diamond, J. Haas, S. Hagopian, V. Hagopian, K.F. Johnson, A. Khatiwada, H. Prosper, V. Veeraraghavan, M. Weinberg

Florida Institute of Technology, Melbourne, USA

V. Bhopatkar, M. Hohlmann, H. Kalakhety, D. Mareskas-palcek, T. Roy, F. Yumiceva

University of Illinois at Chicago (UIC), Chicago, USA

M.R. Adams, L. Apanasevich, D. Berry, R.R. Betts, I. Bucinskaite, R. Cavanaugh, O. Evdokimov, L. Gauthier, C.E. Gerber, D.J. Hofman, P. Kurt, C. O'Brien, I.D. Sandoval Gonzalez, C. Silkworth, P. Turner, N. Varelas, M. Zakaria

The University of Iowa, Iowa City, USA

B. Bilki⁵⁹, W. Clarida, K. Dilsiz, R.P. Gandrajula, M. Haytmyradov, V. Khristenko, J.-P. Merlo, H. Mermerkaya⁶⁰, A. Mestvirishvili, A. Moeller, J. Nachtman, H. Ogul, Y. Onel, F. Ozok⁵⁰, A. Penzo, S. Sen, C. Snyder, P. Tan, E. Tiras, J. Wetzel, K. Yi

Johns Hopkins University, Baltimore, USA

I. Anderson, B.A. Barnett, B. Blumenfeld, D. Fehling, L. Feng, A.V. Gritsan, P. Maksimovic, C. Martin, K. Nash, M. Osherson, M. Swartz, M. Xiao, Y. Xin

The University of Kansas, Lawrence, USA

P. Baringer, A. Bean, G. Benelli, C. Bruner, J. Gray, R.P. Kenny III, D. Majumder, M. Malek, M. Murray, D. Noonan, S. Sanders, R. Stringer, Q. Wang, J.S. Wood

Kansas State University, Manhattan, USA

I. Chakaberia, A. Ivanov, K. Kaadze, S. Khalil, M. Makouski, Y. Maravin, L.K. Saini, N. Skhirtladze, I. Svintradze

Lawrence Livermore National Laboratory, Livermore, USA

D. Lange, F. Rebassoo, D. Wright

University of Maryland, College Park, USA

C. Anelli, A. Baden, O. Baron, A. Belloni, B. Calvert, S.C. Eno, J.A. Gomez, N.J. Hadley, S. Jabeen, R.G. Kellogg, T. Kolberg, Y. Lu, A.C. Mignerey, K. Pedro, Y.H. Shin, A. Skuja, M.B. Tonjes, S.C. Tonwar

Massachusetts Institute of Technology, Cambridge, USA

A. Apyan, R. Barbieri, A. Baty, K. Bierwagen, S. Brandt, W. Busza, I.A. Cali, L. Di Matteo, G. Gomez Ceballos, M. Goncharov, D. Gulhan, M. Klute, Y.S. Lai, Y.-J. Lee, A. Levin, P.D. Luckey, C. McGinn, X. Niu, C. Paus, D. Ralph, C. Roland, G. Roland, G.S.F. Stephans, K. Sumorok, M. Varma, D. Velicanu, J. Veverka, J. Wang, T.W. Wang, B. Wyslouch, M. Yang, V. Zhukova

University of Minnesota, Minneapolis, USA

B. Dahmes, A. Finkel, A. Gude, S.C. Kao, K. Klapoetke, Y. Kubota, J. Mans, S. Nourbakhsh, R. Rusack, N. Tambe, J. Turkewitz

University of Mississippi, Oxford, USA

J.G. Acosta, S. Oliveros

University of Nebraska-Lincoln, Lincoln, USA

E. Avdeeva, K. Bloom, S. Bose, D.R. Claes, A. Dominguez, C. Fangmeier, R. Gonzalez Suarez,

R. Kamalieddin, J. Keller, D. Knowlton, I. Kravchenko, J. Lazo-Flores, F. Meier, J. Monroy, F. Ratnikov, G.R. Snow

State University of New York at Buffalo, Buffalo, USA

M. Alyari, J. Dolen, J. George, A. Godshalk, I. Iashvili, J. Kaisen, A. Kharchilava, A. Kumar, S. Rappoccio

Northeastern University, Boston, USA

G. Alverson, E. Barberis, D. Baumgartel, M. Chasco, A. Hortiangtham, A. Massironi, D.M. Morse, D. Nash, T. Orimoto, R. Teixeira De Lima, D. Trocino, R.-J. Wang, D. Wood, J. Zhang

Northwestern University, Evanston, USA

K.A. Hahn, A. Kubik, N. Mucia, N. Odell, B. Pollack, A. Pozdnyakov, M. Schmitt, S. Stoynev, K. Sung, M. Trovato, M. Velasco, S. Won

University of Notre Dame, Notre Dame, USA

A. Brinkerhoff, N. Dev, M. Hildreth, C. Jessop, D.J. Karmgard, N. Kellams, K. Lannon, S. Lynch, N. Marinelli, F. Meng, C. Mueller, Y. Musienko³², T. Pearson, M. Planer, R. Ruchti, G. Smith, N. Valls, M. Wayne, M. Wolf, A. Woodard

The Ohio State University, Columbus, USA

L. Antonelli, J. Brinson, B. Bylsma, L.S. Durkin, S. Flowers, A. Hart, C. Hill, R. Hughes, K. Kotov, T.Y. Ling, B. Liu, W. Luo, D. Puigh, M. Rodenburg, B.L. Winer, H.W. Wulsin

Princeton University, Princeton, USA

O. Driga, P. Elmer, J. Hardenbrook, P. Hebda, S.A. Koay, P. Lujan, D. Marlow, T. Medvedeva, M. Mooney, J. Olsen, P. Piroué, X. Quan, H. Saka, D. Stickland, C. Tully, J.S. Werner, A. Zuranski

Purdue University, West Lafayette, USA

V.E. Barnes, D. Benedetti, D. Bortoletto, L. Gutay, M.K. Jha, M. Jones, K. Jung, M. Kress, N. Leonardo, D.H. Miller, N. Neumeister, F. Primavera, B.C. Radburn-Smith, X. Shi, I. Shipsey, D. Silvers, J. Sun, A. Svyatkovskiy, F. Wang, W. Xie, L. Xu, J. Zablocki

Purdue University Calumet, Hammond, USA

N. Parashar, J. Stupak

Rice University, Houston, USA

A. Adair, B. Akgun, Z. Chen, K.M. Ecklund, F.J.M. Geurts, W. Li, B. Michlin, M. Northup, B.P. Padley, R. Redjimi, J. Roberts, Z. Tu, J. Zabel

University of Rochester, Rochester, USA

B. Betchart, A. Bodek, P. de Barbaro, R. Demina, Y. Eshaq, T. Ferbel, M. Galanti, A. Garcia-Bellido, P. Goldenzweig, J. Han, A. Harel, O. Hindrichs, A. Khukhunaishvili, G. Petrillo, M. Verzetti, D. Vishnevskiy

The Rockefeller University, New York, USA

L. Demortier

Rutgers, The State University of New Jersey, Piscataway, USA

S. Arora, A. Barker, J.P. Chou, C. Contreras-Campana, E. Contreras-Campana, D. Duggan, D. Ferencek, Y. Gershtein, R. Gray, E. Halkiadakis, D. Hidas, E. Hughes, S. Kaplan, R. Kunnawalkam Elayavalli, A. Lath, S. Panwalkar, M. Park, S. Salur, S. Schnetzer, D. Sheffield, S. Somalwar, R. Stone, S. Thomas, P. Thomassen, M. Walker

University of Tennessee, Knoxville, USA

M. Foerster, K. Rose, S. Spanier, A. York

Texas A&M University, College Station, USA

O. Bouhali⁶¹, A. Castaneda Hernandez, M. Dalchenko, M. De Mattia, A. Delgado, S. Dildick, R. Eusebi, W. Flanagan, J. Gilmore, T. Kamon⁶², V. Krutelyov, R. Montalvo, R. Mueller, I. Osipenkov, Y. Pakhotin, R. Patel, A. Perloff, J. Roe, A. Rose, A. Safonov, I. Suarez, A. Tatarinov, K.A. Ulmer

Texas Tech University, Lubbock, USA

N. Akchurin, C. Cowden, J. Damgov, C. Dragoiu, P.R. Duerdo, J. Faulkner, K. Kovitangoon, S. Kunori, K. Lamichhane, S.W. Lee, T. Libeiro, S. Undleeb, I. Volobouev

Vanderbilt University, Nashville, USA

E. Appelt, A.G. Delannoy, S. Greene, A. Gurrola, R. Janjam, W. Johns, C. Maguire, Y. Mao, A. Melo, P. Sheldon, B. Snook, S. Tuo, J. Velkovska, Q. Xu

University of Virginia, Charlottesville, USA

M.W. Arenton, S. Boutle, B. Cox, B. Francis, J. Goodell, R. Hirosky, A. Ledovskoy, H. Li, C. Lin, C. Neu, E. Wolfe, J. Wood, F. Xia

Wayne State University, Detroit, USA

C. Clarke, R. Harr, P.E. Karchin, C. Kottachchi Kankanamge Don, P. Lamichhane, J. Sturdy

University of Wisconsin, Madison, USA

D.A. Belknap, D. Carlsmith, M. Cepeda, A. Christian, S. Dasu, L. Dodd, S. Duric, E. Friis, R. Hall-Wilton, M. Herndon, A. Hervé, P. Klabbers, A. Lanaro, A. Levine, K. Long, R. Loveless, A. Mohapatra, I. Ojalvo, T. Perry, G.A. Pierro, G. Polese, I. Ross, T. Ruggles, T. Sarangi, A. Savin, N. Smith, W.H. Smith, D. Taylor, N. Woods

†: Deceased

1: Also at Vienna University of Technology, Vienna, Austria

2: Also at CERN, European Organization for Nuclear Research, Geneva, Switzerland

3: Also at Institut Pluridisciplinaire Hubert Curien, Université de Strasbourg, Université de Haute Alsace Mulhouse, CNRS/IN2P3, Strasbourg, France

4: Also at National Institute of Chemical Physics and Biophysics, Tallinn, Estonia

5: Also at Skobeltsyn Institute of Nuclear Physics, Lomonosov Moscow State University, Moscow, Russia

6: Also at Universidade Estadual de Campinas, Campinas, Brazil

7: Also at Laboratoire Leprince-Ringuet, Ecole Polytechnique, IN2P3-CNRS, Palaiseau, France

8: Also at Université Libre de Bruxelles, Bruxelles, Belgium

9: Also at Joint Institute for Nuclear Research, Dubna, Russia

10: Also at Ain Shams University, Cairo, Egypt

11: Also at Suez University, Suez, Egypt

12: Also at Cairo University, Cairo, Egypt

13: Also at Fayoum University, El-Fayoum, Egypt

14: Also at British University in Egypt, Cairo, Egypt

15: Also at Université de Haute Alsace, Mulhouse, France

16: Also at Ilia State University, Tbilisi, Georgia

17: Also at Brandenburg University of Technology, Cottbus, Germany

18: Also at Institute of Nuclear Research ATOMKI, Debrecen, Hungary

19: Also at Eötvös Loránd University, Budapest, Hungary

20: Also at University of Debrecen, Debrecen, Hungary

-
- 21: Also at Wigner Research Centre for Physics, Budapest, Hungary
 - 22: Also at University of Visva-Bharati, Santiniketan, India
 - 23: Now at King Abdulaziz University, Jeddah, Saudi Arabia
 - 24: Also at University of Ruhuna, Matara, Sri Lanka
 - 25: Also at Isfahan University of Technology, Isfahan, Iran
 - 26: Also at University of Tehran, Department of Engineering Science, Tehran, Iran
 - 27: Also at Plasma Physics Research Center, Science and Research Branch, Islamic Azad University, Tehran, Iran
 - 28: Also at Università degli Studi di Siena, Siena, Italy
 - 29: Also at Centre National de la Recherche Scientifique (CNRS) - IN2P3, Paris, France
 - 30: Also at Purdue University, West Lafayette, USA
 - 31: Also at International Islamic University of Malaysia, Kuala Lumpur, Malaysia
 - 32: Also at Institute for Nuclear Research, Moscow, Russia
 - 33: Also at Institute of High Energy Physics and Informatization, Tbilisi State University, Tbilisi, Georgia
 - 34: Also at St. Petersburg State Polytechnical University, St. Petersburg, Russia
 - 35: Also at National Research Nuclear University 'Moscow Engineering Physics Institute' (MEPhI), Moscow, Russia
 - 36: Also at Faculty of Physics, University of Belgrade, Belgrade, Serbia
 - 37: Also at Facoltà Ingegneria, Università di Roma, Roma, Italy
 - 38: Also at Scuola Normale e Sezione dell'INFN, Pisa, Italy
 - 39: Also at University of Athens, Athens, Greece
 - 40: Also at Warsaw University of Technology, Institute of Electronic Systems, Warsaw, Poland
 - 41: Also at Institute for Theoretical and Experimental Physics, Moscow, Russia
 - 42: Also at Albert Einstein Center for Fundamental Physics, Bern, Switzerland
 - 43: Also at Adiyaman University, Adiyaman, Turkey
 - 44: Also at Mersin University, Mersin, Turkey
 - 45: Also at Cag University, Mersin, Turkey
 - 46: Also at Piri Reis University, Istanbul, Turkey
 - 47: Also at Gaziosmanpasa University, Tokat, Turkey
 - 48: Also at Ozyegin University, Istanbul, Turkey
 - 49: Also at Izmir Institute of Technology, Izmir, Turkey
 - 50: Also at Mimar Sinan University, Istanbul, Istanbul, Turkey
 - 51: Also at Marmara University, Istanbul, Turkey
 - 52: Also at Kafkas University, Kars, Turkey
 - 53: Also at Yildiz Technical University, Istanbul, Turkey
 - 54: Also at Kahramanmaras Sütcü Imam University, Kahramanmaras, Turkey
 - 55: Also at Rutherford Appleton Laboratory, Didcot, United Kingdom
 - 56: Also at School of Physics and Astronomy, University of Southampton, Southampton, United Kingdom
 - 57: Also at Utah Valley University, Orem, USA
 - 58: Also at University of Belgrade, Faculty of Physics and Vinca Institute of Nuclear Sciences, Belgrade, Serbia
 - 59: Also at Argonne National Laboratory, Argonne, USA
 - 60: Also at Erzincan University, Erzincan, Turkey
 - 61: Also at Texas A&M University at Qatar, Doha, Qatar
 - 62: Also at Kyungpook National University, Daegu, Korea